بسم الله الرحمن الرحيم

BACHELOR OF SCIENCE IN ELECTRICAL AND ELECTRONIC ENGINEERING

OPTICAL FIBER FOR TERAHERTZ WAVE

By

JAMILUR RAHMAN (122476)

MD. ABDUR RAFI (122420)

MD. ASHFAQ UDDIN (122417)

Supervised by

Prof. Dr. Mohammad Rakibul Islam

Department of Electrical and Electronic Engineering

Islamic University of Technology (IUT)

November, 2016

Contents

List of Figures

ACKNOWLEDGEMENTS

The first thank and honor go to the Almighty. He has given us the capability and opportunity to finish this work perfectly. We have tried our best through the whole year and this research is our most significant scientific accomplishment in our educational life. But, without His help, it would not be possible for us.

After that, we would like to thank our honorable respective supervisor, Prof. Dr. Mohammad Rakibul Islam for his guidance, motivation and help during the thesis work. He has worked very hard and helped us a lot to finish and finalize this research work.

We would also like to thank other respective teachers, our friends and family members for their support and motivation which were also the key points behind our success.

Abstract

Terahertz radiation occupies a middle ground between microwaves and infrared light waves known as the terahertz gap, where technology for its generation and manipulation is in its infancy. The frequency band of 0.1-10 THz, known as THz band has brought potential applications in many important fields.

For wave propagation THz systems use free space as medium. But in free space waves face many difficulties which is very big issue for wave propagation. So we have to use guided transmission instead of unguided transmission.

In the mean time many guided transmission line has many kinds of deprivation such as effective material loss, confinement loss, bending loss, dispersion loss, power fraction issue etc.

So we had decided to make a porous core fiber which has less losses than other PCF. Mainly we have been inspired from previous papers in which these losses was too much high for THz wave guidance.

Then we have designed rotate hexagonal core and decagonal cladding with 8% PML of total fiber radius. This design gives a lower effective material loss and comparatively higher mode power propagation as well as a flattened dispersion gained over the frequency range 0.95-1.25 THz.

CHAPTER 1

What Is Optical fiber Communication

1.1 Optical Fiber Communication

Fiber optic communication is a communication technology that uses light pulses to transfer information from one point to another through an optical fiber. The information transmitted is essentially digital information generated by telephone systems, cable television companies, and computer systems.

1.2 EVOLUTION OF FIBER OPTICS COMMUNICATION

1.2.1 Background

Optical fiber was first developed in 1970 by Corning Glass Works. At the same time, GaAs semiconductor lasers were also developed for transmitting light through the fiber optic cables. The first generation fiber optic system was developed in 1975, it used GaAs semiconductor lasers, operated at a wavelength of 0.8 μm, and bit rate of 45Megabits/second with 10Km repeater spacing.

In the early 1980's, the second generation of fiber optic communication was developed, it used InGaAsP semiconductor lasers and operated at a wavelength of 1.3 μm.

By 1987, these fiber optic systems were operating at bit rates of up to 1.7 Gigabits/second on single mode fiber with 50Km repeater spacing.

1.2.2 3rd Generation

The third generation of fiber optic communication operating at a wavelength of 1.55 μm was developed in 1990. These systems were operating at a bit rate of up to 2.5 Gigabits/second on a single longitudinal mode fiber with 100Km repeater spacing.

1.2.3 4th Generation

The fourth generation of fiber optic systems made use of optical amplifiers as a replacement for repeaters, and utilized wavelength division multiplexing (WDM) to increase data rates. By 1996, transmission of over 11,300Km at a data rate of 5Gigabits/second had been demonstrated using submarine cables.

1.2.4 5th Generation

The fifth generation fiber optic communication systems use the Dense Wave Division Multiplexing (DWDM) to further increase data rates. Also, the concept of optical solitons, which are pulses that can preserve their shape by counteracting the negative effects of dispersion, is also being explored.

1.3 Ingredients

The major driving force behind the widespread use of fiber optics communication is the high and rapidly increasing consumer and commercial demand for more telecommunication capacity and internet services, with fiber optic technology capable of providing the required information capacity (larger than both wireless connections and copper cable). Advances in technology have enabled more data to be conveyed through a single optical fiber over long distances. The transmission capacity in optical communication networks are significantly improved using wavelength division multiplexing.

1.4 Mechanism

An optical network has the ability to process information entirely in the optical domain for the purpose of amplification, multiplexing, de-multiplexing, switching, filtering, and correlation, since optical signal processing is more efficient than electrical signal processing. Code Division Multiple Access networks using optical signal processing techniques have recently being introduced.

1.5 Optical fiber waveguide

An optical fiber is a dielectric cylindrical waveguide made from low-loss materials, usually silicon dioxide. The core of the waveguide has a refractive index a little higher than that of the outer medium (cladding), so that light pulses is guided along the axis of the fiber by total internal reflection.

1.6 Transmission through fiber

Fiber optic communication systems consists of an optical transmitter to convert an electrical signal to an optical signal for transmission through the optical fiber, a cable containing several bundles of optical fibers, optical amplifiers to boost the power of the optical signal, and an optical receiver to reconvert the received optical signal back to the original transmitted electrical signal.

1.7 Basic Optical Fiber Communication

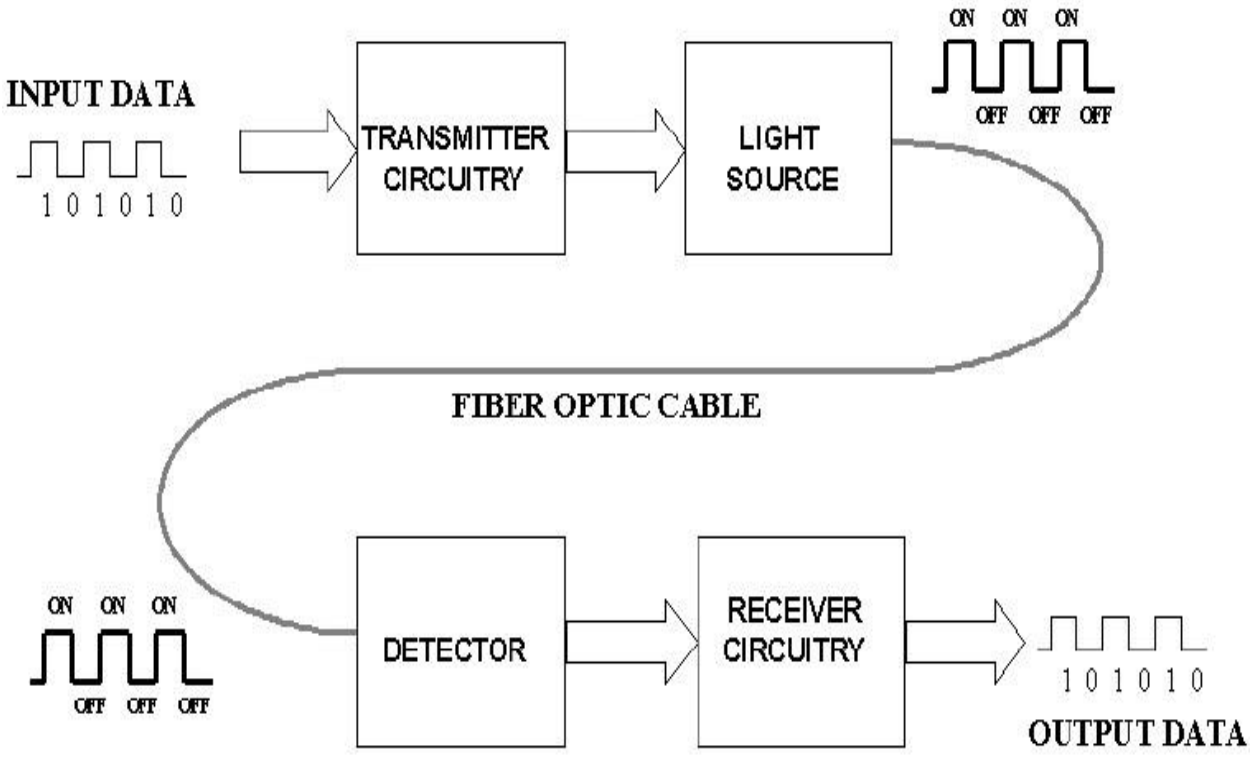

Fig 1.1: Basic fiber optic communication system

Figure 1.1 gives a simplified description of a basic fiber optic communication system.

1.8 Categories of Optical Fiber

Optical fibers fall into two major categories, namely:

- Step index optical fiber
- Graded index optical fiber

1.8.1 Step index optical fiber

Step index optical fiber, which include single mode optical fiber and multimode optical fiber, and graded index optical fiber. Single mode step index optical fiber has a core diameter less than 10 micrometers and only allows one light path. Multimode step index optical fiber has a core diameter greater than or equal to 50 micrometers and allows several light paths, this leads to modal dispersion.

1.8.2 Graded index optical fiber

Graded index optical fibers have their core refractive index gradually decrease farther from the centre of the core, this increased refraction at the core centre slows the speed of some light rays, thereby allowing all the light rays to reach the receiver at almost the same time, thereby reducing dispersion.

1.9 Various Categories Fiber Mode

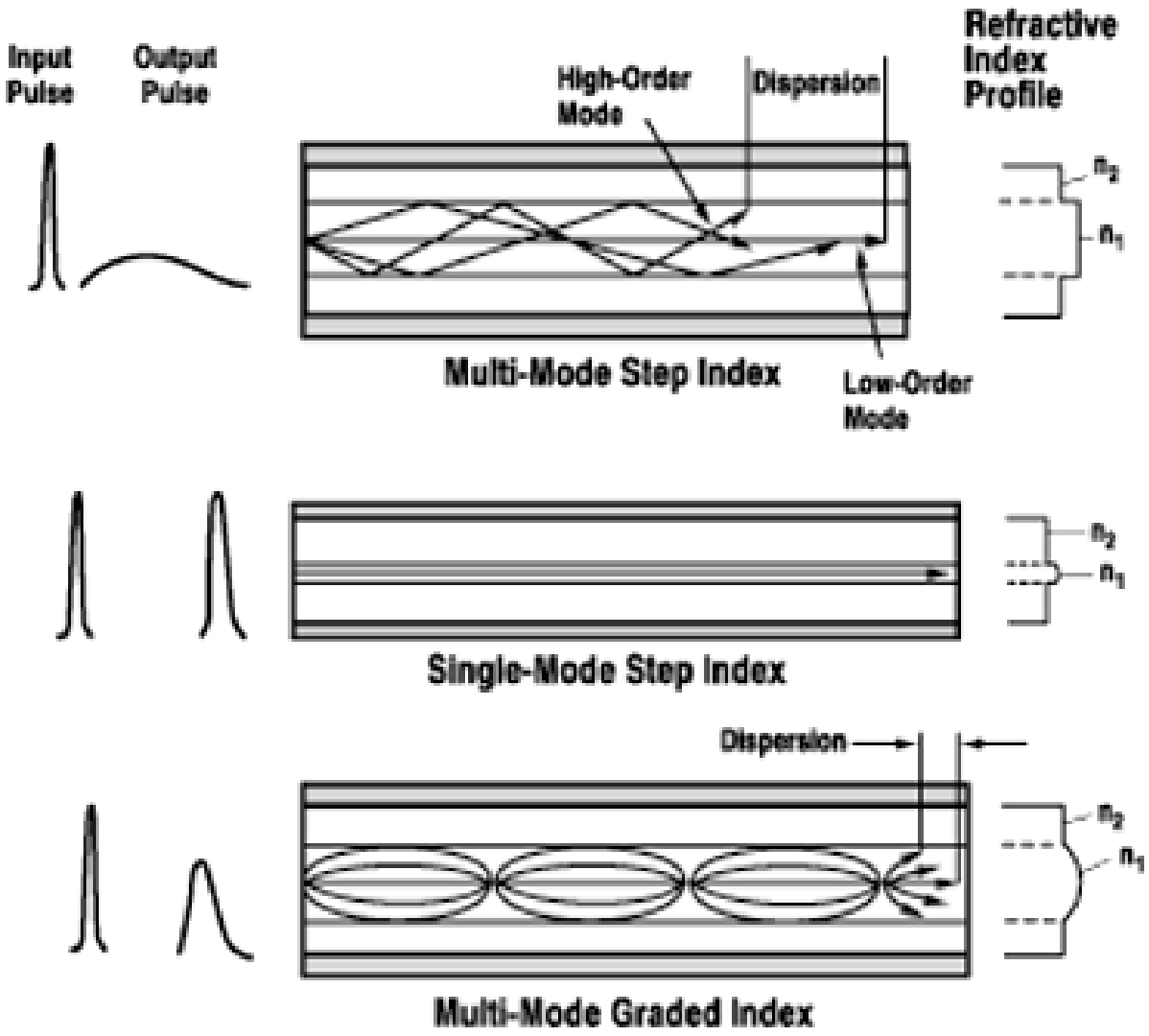

Fig 1.2: Optical Fiber Modes

Figure 1.2 gives a description of the various optical fiber modes.

1.10 Basic Steps

The process of communicating using fiber-optics involves the following basic steps:

1. creating the optical signal involving the use of a transmitter, usually from an electrical signal
2. relaying the signal along the fiber, ensuring that the signal does not become too distorted or weak
3. receiving the optical signal
4. converting it into an electrical signal

1.11 Technology

Modern fiber-optic communication systems generally include an optical transmitter to convert an electrical signal into an optical signal to send into the optical fiber, a cable containing bundles of multiple optical fibers that is routed through underground conduits and buildings, multiple kinds of amplifiers, and an optical receiver to recover the signal as an electrical signal. The information transmitted is typically digital information generated by computers, telephone systems, and cable television companies.

1.12 Transmitters

The most commonly used optical transmitters are semiconductor devices such as light-emitting diodes (LEDs) and laser diodes. The difference between LEDs and laser diodes is that LEDs produce incoherent light, while laser diodes produce coherent light. For use in optical communications, semiconductor optical transmitters must be designed to be compact, efficient, and reliable, while operating in an optimal wavelength range, and directly modulated at high frequencies.

1.13 LED

In its simplest form, an LED is a forward-biased p-n junction, emitting light through spontaneous emission, a phenomenon referred to as electroluminescence. The emitted light is incoherent with a relatively wide spectral width of 30-60 nm. LED light transmission is also inefficient, with only about 1% of input power, or about 100 microwatts, eventually converted into launched power which has been coupled into the optical fiber. However, due to their relatively simple design, LEDs are very useful for low-cost applications.

Today, LEDs have been largely superseded by VCSEL (Vertical Cavity Surface Emitting Laser) devices, which offer improved speed, power and spectral properties, at a similar cost. Common VCSEL devices couple well to multimode fiber.

1.14 Receivers

The main component of an optical receiver is a photodetector, which converts light into electricity using the photoelectric effect. The primary photodetectors for telecommunications are made from Indium gallium arsenide. The photo detector is typically a semiconductor-based photodiode. Several types of photodiodes include p-n photodiodes, p-i-n photodiodes, and avalanche photodiodes. Metal-semiconductor-metal (MSM) photo detectors are also used due to their suitability for circuit integration in regenerators and wavelength-division multiplexers.

Optical-electrical converters are typically coupled with a trans-impedance amplifier and a limiting amplifier to produce a digital signal in the electrical domain from the incoming optical signal, which may be attenuated and distorted while passing through the channel. Further signal processing such as clock recovery from data (CDR) performed by a phase-locked loop may also be applied before the data is passed on.

1.15 Transceiver

A transceiver is a device combining a transmitter and a receiver in a single housing.

Most systems use a "transceiver" which includes both transmission and receiver in a single module. The transmitter takes an electrical input and converts it to an optical output from a laser diode or LED. The light from the transmitter is coupled into the fiber with a connector and is transmitted through the fiber optic cable plant. The light from the end of the fiber is coupled to a receiver where a detector converts the light into an electrical signal which is then conditioned properly for use by the receiving equipment.

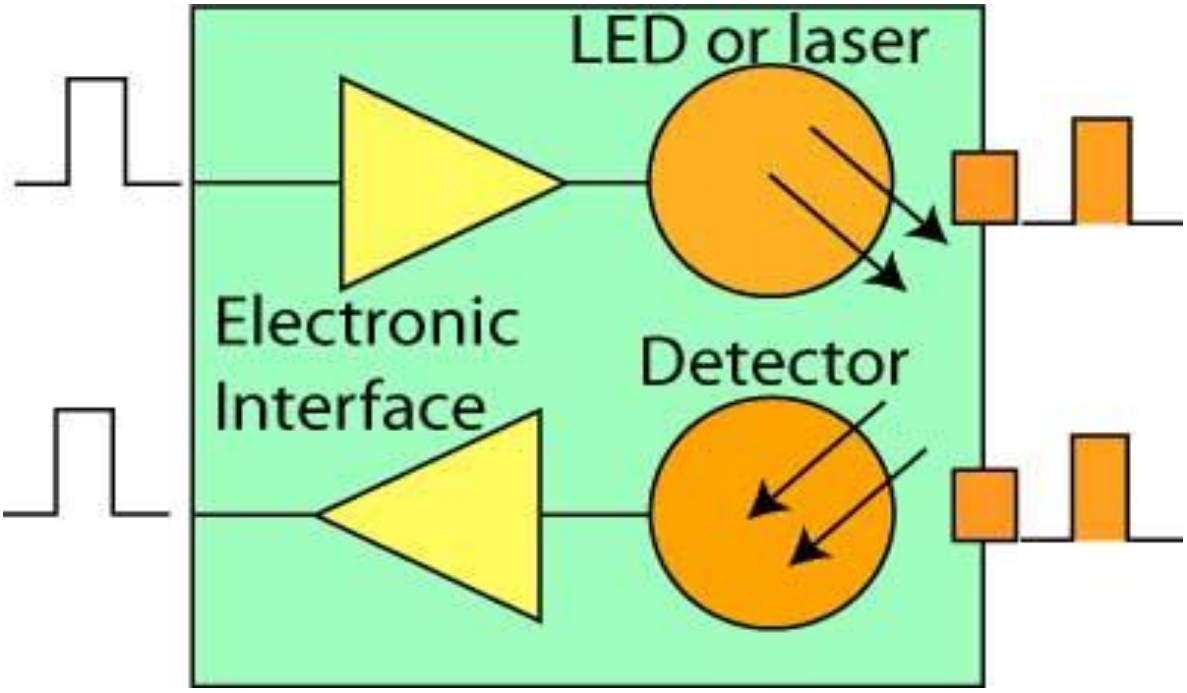

Fig 1.3: Fiber Optic Transceiver

1.16 Amplifier

The transmission distance of a fiber-optic communication system has traditionally been limited by fiber attenuation and by fiber distortion. By using opto-electronic repeaters, these problems have been eliminated. These repeaters convert the signal into an electrical signal, and then use a transmitter to send the signal again at a higher intensity than was received, thus counteracting the loss incurred in the previous segment. Because of the high complexity with modern wavelength-division multiplexed signals (including the fact that they had to be installed about once every 20 km), the cost of these repeaters is very high.

1.17 Wavelength-division multiplexing

Wavelength-division multiplexing (WDM) is the practice of multiplying the available capacity of optical fibers through use of parallel channels, each channel on a dedicated wavelength of light. This requires a wavelength division multiplexer in the transmitting equipment and a demultiplexer (essentially a spectrometer) in the receiving equipment. Arrayed waveguide gratings are commonly used for multiplexing and demultiplexing in WDM. Using WDM technology now commercially available, the bandwidth of a fiber can be divided into as many as 160 channels to support a combined bit rate in the range of 1.6 Tbit/s.

1.18 Applications

Optical fiber is used by many telecommunications companies to transmit telephone signals, Internet communication, and cable television signals. Due to much lower attenuation and interference, optical fiber has large advantages over existing copper wire in long-distance and high-demand applications. However, infrastructure development within cities was relatively difficult and time-consuming, and fiber-optic systems were complex and expensive to install and operate. Due to these difficulties, fiber-optic communication systems have primarily been installed in long-distance applications, where they can be used to their full transmission capacity, offsetting the increased cost. Since 2000, the prices for fiber-optic communications have dropped considerably.

The price for rolling out fiber to the home has currently become more cost-effective than that of rolling out a copper based network. Prices have dropped to $850 per subscriber in the US and lower in countries like The Netherlands, where digging costs are low and housing density is high.

CHAPTER 2

History

In the recent years THz wave generation and detection techniques have already been developed to cope with its popularity. However due to the lack of low loss transmission waveguides in the THz frequencies, most of the THz systems depends on free space for its wave propagation since all the remaining waveguides are extremely absorbent in this frequency band. Propagation in free space faces some undesirable problems. These include a tough configuration, path loss, an uncertain absorption loss influenced by the atmosphere, and difficult integration with other components. Therefore, transmissions of THz waves for long distance are still in the demanding state.

Therefore much effort has been given for its solutions, one can be to use optical fiber where there is no influence of external free space, these can dramatically reduce the losses and alignment problems also the system performances can also be increased.

2.1 Introduction To Terahertz

The TERAHERTZ (THz) frequency/wavelength window of the electro-magnetic spectrum lies between the infrared band and the microwave band and ranges in frequency from 0.1 to 10 THz (equivalently wavelength ranges from 3 mm – 30 μm). Radiation from any object with temperature > 10 K contains THz wavelengths and almost 98% of cosmic background radiations since Big-Bang event corresponds to THz and far-infrared frequencies. Initially THz radiation was mainly used for passive applications, where THz waves were detected to study the chemistry of cold planetary atmosphere and interstellar medium.

2.1.1 Why Researchers decided to use this gap

This frequency range can transfer huge data files via wireless route and can significantly increase the communication data rate over existing microwave technology. THz waves can deeply penetrate through cloths, ceramics, walls, woods, paper, dry air, polymers etc., but they are absorbed or reflected by metal, water vapor, dust, cloud, and sufficiently dense objects. Additionally, THz waves are also not harmful to human health. All these excellent qualities of THz radiation make it suitable for imaging of hidden objects, like explosives, metallic weapons etc. Most importantly, this technology has already begun to make deep inroads in non-invasive medical diagnostics, such as detection of skin cancer, tooth decay, and identification of human tissues based on different refractive indices and linear absorption coefficients at THz frequencies.

2.2 Wave Propagation

Since most of the THz systems and THz communication experiments are bulky and are performed in free space, it faces many undesirable problems. These include a tough transmitter-receiver alignment issues, an uncertain absorption loss influenced by the surroundings and difficult integration with other components.

2.2.1 Guided Transmission

To overcome these problems, researchers proposed guided transmission instead of unguided transmission. Researchers showed that the THz wave can nicely be propagated through all kinds of conventional metallic waveguides.

2.3 Background of THz Waveguides

2.3.1 Auston Switch

In the early 1980s, THz pulses (in the pico/sub picosecond regime) were generated and sampled by photoconductive switches, also known as Auston switches. These photoconductive switches were incorporated into microstrip and coplanar (still used today) transmission lines.

2.3.2 Microstrip

A microstrip transmission line is a type of electrical transmission line that consists of a conducting strip separated from a ground plane by a dielectric substrate, while a coplanar transmission line is an alternative type of electrical transmission line that consists of a conducting strip on a dielectric substrate with two ground electrodes running adjacent and parallel to strip.

2.3.3 Limitation of Microstrip

A limitation of the microstrip line configuration, in the THz system, was that such systems suffered from reflections (ringing) at the generation point. Also these microstrip based THz systems had high dispersion due to the dielectric substrate.

2.3.4 Coplanar

In the coplanar transmission THz system, the generated sub picosecond pulse (0.6 ps, for example) undergoes lower distortion compared to microstrip lines. Therefore, they are more suitable for far-IR spectroscopy.

2.3.5 Limitation Of Coplanar

The coplanar transmission line THz system suffers from strong frequency dependent loss due to Cherenkov-like radiation, which is equivalent to the loss process of leaky waveguides in the frequency domain. The total observed loss owing to the dielectric and metal in microstrip and coplanar transmission lines in THz systems is very high.

2.3.6 Reported Losses

For thin-film microstrip and coplanar transmission lines are $\alpha = 18\ cm^{-1}$ and $\alpha = 14\ cm^{-1}$ at 1 THz, respectively. The loss increases as frequency increases with f and f^3 dependence, respectively.

2.3.7 Circular Metallic Waveguide

Initially, to propagate THz wave researchers used Circular metallic waveguide [1] like stainless solid but these waveguide are highly lossy on the order of 50 DB/cm. Although a THz wave cannot be guided inside a hollow dielectric tube, if this tube is coated with a metal layer, a plasmonic mode can form inside the hollow core, where the guiding environment can be better controlled or manipulated.

2.3.8 Additional Thin Dielectric Layer

It has been observed that by incorporating an additional thin dielectric layer [2], the mode field can be drawn away from the lossy plasmonic interface and, as a consequence, the overall loss value can be reduced [3]. However, these waveguides are not very flexible for large diameter waveguides and increase the loss value for small diameter waveguides.

2.3.9 Hollow Core Fiber

Hollow dielectric tubes [4] coated with metal layer were reported, but they appeared to be bulky.

2.3.10 Low Index Dry Index

To overcome these obstacles, one usually designs various kinds of waveguides to guide the THz wave because the material absorption loss is high in THz band. One of the lowest material loss materials is dry air in the THz frequency range. It has been reported [5] that the mode field extends into the low index air cladding region when a dielectric rod is surrounded by air and is operating very close to its cutoff frequency. The main disadvantage of this design is that the mode extends considerably into the surrounding air cladding and the power is propagated mostly outside the waveguide, which strongly interacts with the surrounding environment. As a result, the bending loss would also be expected to be excessively high.

2.3.11 Plastic sub wavelength fibers

Plastic sub wavelength fibers [6] came into existence for their comparatively lower losses. However, there is a disadvantage for the sub-wavelength fibers that most of the field propagates outside the waveguide core, thus resulting in strong coupling to the environment.

For improvement, Nagel et al. [7] reported the addition of a sub-wavelength hole within a solid core, which increases the guided field in the air hole and hence reducing the absorption losses. However, the loss due to the material is still high.

2.4 Use of Polymers

Interest of researchers shifted from dielectrics to polymers when Chen et al. [8] showed that polyethylene can be used as a guidance material which has lower absorption loss. In recent times, variety of polymers such as Poly methyl Methacrylate (PMMA) [9], TOPAS [10], Teflon [11] etc. are being used as primary choices for THz wave guiding.

In order to reduce absorption loss further, researchers put their attention into guiding structure designing. Dry air is assumed to have no material absorption loss at THz frequency range. On the basis of that, wave guide with sub-wavelength air hole in the core was reported [8]. However, it caused huge power dissipation outside the guide. Later, polystyrene foam was introduced [12] which had a major disadvantage that it required larger dimension.

Actually, genuine breakthrough of the research works occurred when polymer materials were used instead of metals in the background which represent a much lower absorption loss.

2.4.1 Hollow core Bragg Fiber

Hollow core Bragg fibers [13-14] have also been considered which, unfortunately, had unwanted narrow band properties.

2.4.2 Photonic Crystal Fiber

Photonic crystal fiber (PCF) is the most popular optical fiber but in case of a solid core [15], the material absorption loss is too high and is almost equal to the bulk absorption loss of the material.

In a PCF, light is guided through the waveguide using total internal reflection property based on the difference between refractive indices of the core and the cladding. In general, the cladding is consisted of a number of air holes [16]. Recently, PCFs have been popular for their modification enabled property which helps controlling their behavior. Although, solid core polymer-made PCFs had been introduced for THz wave guiding, [11, 17] they could not create a spark because the solid core caused significant amount of loss. As an attempt, air filling ratio was extremely increased to force the light through air holes of the cladding [18-19], but size of the waveguide got enlarged.

2.5 Use of Porous air core in PCF

Implementing porous air core in a PCF instead of solid rod came out as a solution. Use of a porous core is resulted in reduction of quantity of solid material in the core as well as the absorption loss.

2.5.1 Honeycomb Band-gap Fibers

Efficient honeycomb band-gap fibers were reported [20-21], where porous core PCFs were investigated both numerically and experimentally. Also, a hexagonal PCF with hexagonal porous core was reported [22] with a low absorption loss (0.12 cm^{-1}) where Teflon was used as the background material.

2.5.2 Sub-wavelength Porous Fibers

The sub-wavelength porous fibers have been proven to exhibit some merits namely extremely low loss, design and fabrication flexibilities, and small fiber diameters [23]. Moreover, dispersion of the porous fibers can be controlled easily. In such fibers, owing to the sub-wavelength diameter of the core, the fundamental guided mode presents surrounding the air-cladding and hence low absorption loss is obtained [24].

2.5.3 Use of TOPAS

A better approach with TOPAS was presented which had an octagonal porous core inside an octagonal cladding [25] with a lower loss (0.07 cm^{-1}) resulted due to the lower bulk material absorption loss of TOPAS. Nevertheless, the paper had no discussion on power fraction or dispersion properties.

CHAPTER 3

BACKGROUND

Various porous core PCFs with noticeable material loss properties were reported over the ages.

A microstructure core honeycomb band-gap fiber for THz wave guidance was reported by Neilsen et al. [26] but in this case periodicity still needs to be maintained strictly in narrowband fibers to satisfy the Bragg conditions.

A porous core fiber with TOPAS as background material using hexagonal structure in both core and cladding was reported by Uthman et al. [27] reported which showed Effective Material Loss (EML) of 0.12 cm-1 but they didn't mention some important properties for THz applications like dispersion and fraction of power.

A porous core fiber having both flattened dispersion and 80% light confinement within the core area was proposed by Liang et al. [28] Because of having higher absorption loss of 0.432 dB/cm at 1.0 THz, this design has not been so seductive for THz guidance.

Kaijage et al. [29] reported a porous core fiber which warrants effective material loss of 0.076 cm-1 but they did not take into consideration some crucial design issues for THz guidance such as dispersion and core power fraction.

A fiber with hexagonal core and rotate hexagonal cladding was proposed by Islam et al. [30] which showed the EML= 0.066 cm-1 and core power fraction of 0.40.

A fiber with decagonal core and cladding structure was proposed by Rana et al. [31] but it showed a material loss of 0.058 cm-1 and they neglect to investigate the dispersion properties of that fiber.

A fiber with decagonal structure in the cladding and circular structure in the core was proposed by Hasan et al. [32] which showed an effective material loss of 0.056 cm-1 but they didn't even mention the single mode condition which is one of the main properties for analyzing a fiber.

A rotated hexagonal core surrounded by a circular shape cladding was reported by Saiful et al. [33] which gave loss of .053 cm-1 but can be further reduced & thus improve the efficiency.

3.1 Overview of some important background work done in different times

- A polarization maintaining ultra-low effective material loss based on slotted core kagome lattice fiber is proposed for terahertz (THz) wave propagation was proposed by Md Rabiul hasan, Numerical study demonstrates that by using rectangular slotted air holes in the core of the kagome lattice exhibits simultaneously an ultra-high birefringence of 8.22 × 10−2, an ultra-low effective material loss of 0.05 cm−1, and a very low confinement loss of 4.13×10−5 cm−1 at the frequency of 1 THz. Further investigation shows that about half of the total mode power confines into the air slots at 50% core porosity. The proposed fiber can be used for polarization maintaining applications in THz regime.

- A novel porous-core octagonal photonic crystal fiber (POPCF) for practical low-loss terahertz (THz) wave guiding was suggested by Kaijagge. The POPCF with a porous core surrounded by an air-hole cladding shows a low material absorption loss of ∼0.07 cm−1, or one third of that for the bulk material absorption loss at the operating frequency ∼1 THz. In addition, the confinement loss, bending loss, and effective modal area properties of the POPCF are also reported and demonstrated to be relatively low. The proposed POPCF has potential applications for efficient transmission of broadband THz radiation.

- A photonic crystal fiber having ultralow material loss and near-zero dispersion at the telecom window which is suitable for THz wave guidance was proposed by Imran Hasan. The finite element method with perfectly matched layer circular boundary is used to investigate the guiding properties. The numerical results show that ultra-low material absorption loss of 0.056 cm−1 at 1.0 THz and nearly zero flattened dispersion of ±0.18 ps/THz/cm can be obtained from the proposed fiber in the wavelength range of 1.0–1.8 THz.

- This letter reports a photonic crystal fiber having ultralow material loss and near-zero dispersion at the telecom window which is suitable for THz wave guidance. The finite element method with perfectly matched layer circular boundary is used to investigate the guiding properties. The numerical results show that ultra-low material absorption loss of 0.056 cm−1 at 1.0 THz and nearly zero flattened dispersion of ±0.18 ps/THz/cm can be obtained from the proposed fiber in the wavelength range of 1.0–1.8 THz.

- A new type of dielectric 1Hz waveguide, which evolved from a recent approach from the field of integrated optics, is presented with theoretical and experimental results. Due to the continuity of electric flux density at a dielectric interface, the THz wave is predominantly confined in the virtually lossless low index air core of a high-index dielectric waveguide. Attenuation, dispersion, field enhancement and field confinement properties of the waveguide are discussed and compared to those of other THz waveguide approaches.

CHAPTER 4

PHOTONIC CRYSTAL FIBER AND THz BAND

4.1 Photonic-crystal fiber

Photonic-crystal fiber (PCF) is a new class of optical fiber based on the properties of photonic crystals. Because of its ability to confine light in hollow cores or with confinement characteristics not possible in conventional optical fiber, PCF is now finding applications in fiber-optic communications, fiber lasers, nonlinear devices, high-power transmission, highly sensitive gas sensors, and other areas. More specific categories of PCF include photonic-bandgap fiber (PCFs that confine light by band gap effects), holey fiber (PCFs using air holes in their cross-sections), hole-assisted fiber (PCFs guiding light by a conventional higher-index core modified by the presence of air holes), and Bragg fiber (photonic-bandgap fiber formed by concentric rings of multilayer film). Photonic crystal fibers may be considered a subgroup of a more general class of micro-structured optical fibers, where light is guided by structural modifications, and not only by refractive index differences.

4.1.1 Description

Optical fibers have evolved into many forms since the practical breakthroughs that saw their wider introduction in the 1970s as conventional step index fibers and later as single material fibers where propagation was defined by an effective air cladding structure.

In general, regular structured fibers such as photonic crystal fibers, have a cross-section (normally uniform along the fiber length) micro-structured from one, two or more materials, most commonly arranged periodically over much of the cross-section, usually as a "cladding" surrounding a core (or several cores) where light is confined. For example, the fibers first demonstrated by Russell consisted of a hexagonal lattice of air

holes in a silica fiber, with a solid (1996) or hollow (1998) core at the center where light is guided. Other arrangements include concentric rings of two or more materials, first proposed as "Bragg fibers" by Yeh and Yariv (1978), a variant of which was recently fabricated by Temelkuran et al. (2002) and others.

(Note: PCFs and, in particular, Bragg fibers, should not be confused with fiber Bragg gratings, which consist of a periodic refractive index or structural variation along the fiber axis, as opposed to variations in the transverse directions as in PCF. Both PCFs and fiber Bragg gratings employ Bragg diffraction phenomena, albeit in different directions.)

The lowest reported attenuation of solid core photonic crystal fiber is 0.37 dB/km, and for hollow core is 1.2 dB/km.

4.1.2 Construction

Generally, such fibers are constructed by the same methods as other optical fibers: first, one constructs a "preform" on the scale of centimeters in size, and then heats the preform and draws it down to a much smaller diameter (often nearly as small as a human hair), shrinking the preform cross section but (usually) maintaining the same features. In this way, kilometers of fiber can be produced from a single preform. The most common method involves stacking, although drilling/milling was used to produce the first aperiodic designs. This formed the subsequent basis for producing the first soft glass and polymer structured fibers.

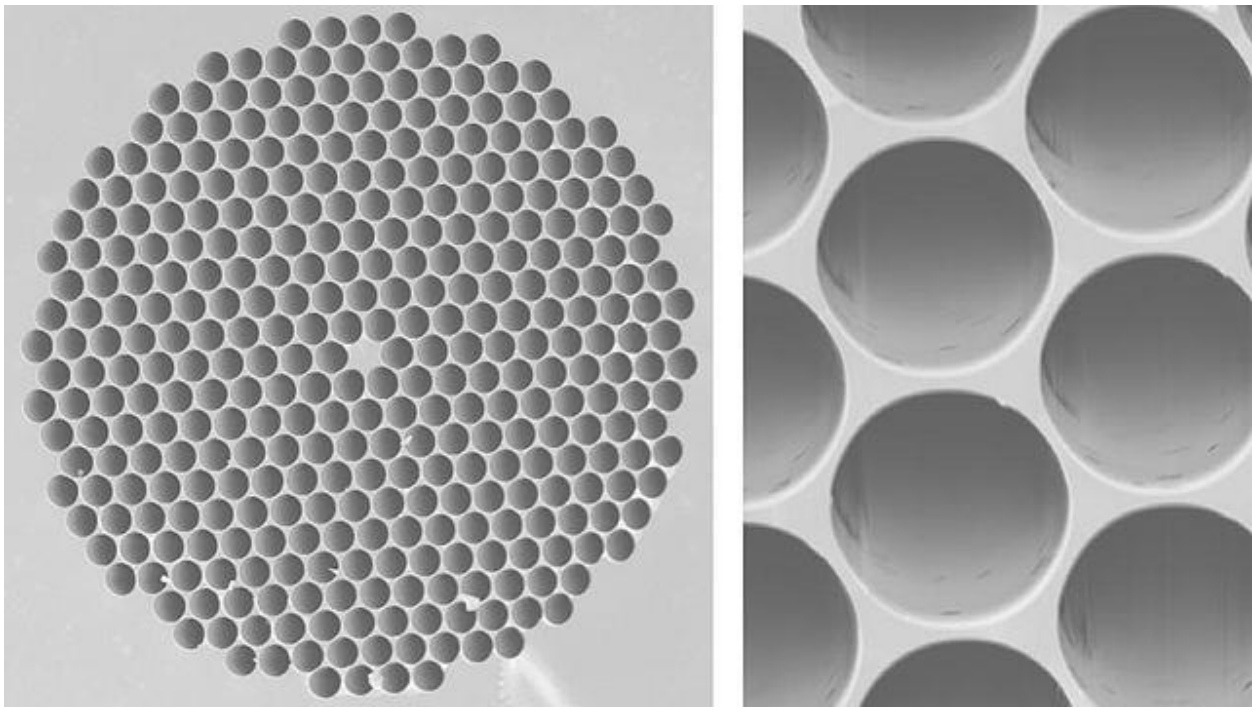

Fig 4.1: Photonic Crystal Fiber

Most photonic crystal fibers have been fabricated in silica glass, but other glasses have also been used to obtain particular optical properties (such as high optical non-linearity). There is also a growing interest in making them from polymer, where a wide variety of structures have been explored, including graded index structures, ring structured fibers and hollow core fibers. These polymer fibers have been termed "MPOF", short for micro-structured polymer optical fibers (van Eijkelenborg, 2001). A combination of a polymer and a chalcogenide glass was used by Temelkuran et al. (2002) for 10.6 μm wavelengths (where silica is not transparent).

4.1.3 Modes of operation

Photonic crystal fibers can be divided into two modes of operation, according to their mechanism for confinement. Those with a solid core, or a core with a higher average index than the micro-structured cladding, can operate on the same index-guiding principle as conventional optical fiber — however, they can have a much higher effective- refractive index contrast between core and cladding, and therefore can have

much stronger confinement for applications in nonlinear optical devices, polarization-maintaining fibers, (or they can also be made with much lower effective index contrast). Alternatively, one can create a "photonic bandgap" fiber, in which the light is confined by a photonic bandgap created by the micro-structured cladding – such a bandgap, properly designed, can confine light in a lower-index core and even a hollow (air) core. Bandgap fibers with hollow cores can potentially circumvent limits imposed by available materials, for example to create fibers that guide light in wavelengths for which transparent materials are not available (because the light is primarily in the air, not in the solid materials). Another potential advantage of a hollow core is that one can dynamically introduce materials into the core, such as a gas that is to be analyzed for the presence of some substance. PCF can also be modified by coating the holes with sol-gels of similar or different index material to enhance its transmittance of light.

4.2 THz Band and its Application

Terahertz radiation falls in between infrared radiation and microwave radiation in the electromagnetic spectrum and it shares some properties with each of these. Like infrared and microwave radiation, terahertz radiation travels in a line of sight and is non-ionizing. Like microwave radiation, terahertz radiation can penetrate a wide variety of non-conducting materials. Terahertz radiation can pass through clothing, paper, cardboard, wood, masonry, plastic and ceramics. The penetration depth is typically less than that of microwave radiation. Terahertz radiation has limited penetration through fog and clouds and cannot penetrate liquid water or metal.

In physics, terahertz radiation, also called submillimeter radiation, terahertz waves, terahertz light, T-rays, T-waves, T-light, T-lux, or THz, consists of electromagnetic waves at frequencies from 0.3 to 10 terahertz (THz). The term applies to electromagnetic radiation with frequencies between the high-frequency edge of the millimeter wave band, 300 GHz and the low frequency edge of the far-infrared light

band, 3000 GHz. Corresponding wavelengths of radiation in this band range from 1 mm to 0.1 mm (or 100 μm). Because terahertz radiation begins at a wavelength of 1 mm and proceeds into shorter wavelengths, it is sometimes known as the submillimeter band and its radiation as submillimeter waves, especially in astronomy.

The earth's atmosphere is a strong absorber of terahertz radiation in specific water vapor absorption bands, as seen in Fig. 1, so the range of terahertz radiation is limited enough to affect its usefulness in long-distance communications. However, at distances of ~10 m the band may still allow many useful applications in imaging and construction of high bandwidth wireless networking systems, especially indoor systems.[3] In addition, producing and detecting coherent terahertz radiation remains technically challenging, though inexpensive commercial sources now exist in the 300–1000 GHz range (the lower part of the spectrum), including gyrotrons, backward wave oscillators, and resonant-tunneling diodes.

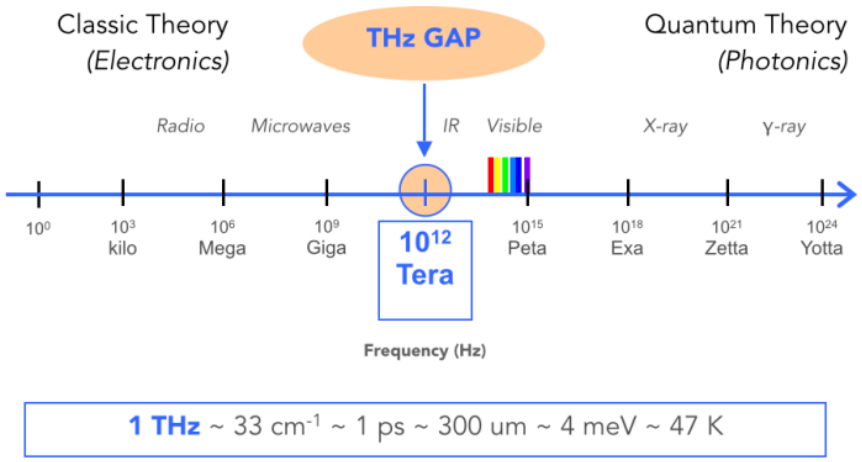

Fig 4.2: THz gap in electromagnetic spectrum

Terahertz radiation occupies a middle ground between microwaves and infrared light waves, and technology for generating and manipulating it is in its infancy and is a subject of active research (Fig. 1). It represents the region in the electromagnetic spectrum in which the frequency of electromagnetic radiation becomes too high to be

measured by directly counting cycles using electronic counters, and must be measured by the proxy properties of wavelength and energy.

Similarly, in this frequency range the generation and modulation of coherent electromagnetic signals ceases to be possible by the conventional electronic devices used to generate radio waves and microwaves, and requires new devices and techniques. The electromagnetic range that is used is very vast. At low frequencies end we have radio waves up to millimeter waves, and at the other end we have optical waves down to the far infrared. Technologies have been developed for both ends of the spectrum which we use in everyday applications. But the terahertz region:

$$0.3 - 10\,\mathrm{THz},\ \ 1\,\mathrm{THz} = 1012\,\mathrm{Hz}$$

With wavelength of 30 μm – 3 mm has remained largely underdeveloped, despite the identification of various applications, in particular terahertz imaging and others which will be discussed later on.

It is possible to produce effectively radiation in the low frequency region (microwaves) with oscillating circuits based on high-speed transistors and at high frequencies (visible spectrum) with semiconductor lasers. But transistors and other electric devices based on electric transport have in principle a limit at about 300 GHz, but are practically limited to about 50 GHz, because devices above this are extremely inefficient and the frequency of semiconductor lasers can only be extended down to about 30 THz. Thus there is a region in between where both technologies do not meet. This region is often referred to as the terahertz gap.

Terahertz radiations have a few remarkable properties. Many common materials and living tissues are semitransparent and have ‘terahertz fingerprints’, permitting them to be imaged, identified and analyzed. Due to non-ionizing properties of terahertz radiations are safe for screening application. These unique properties of radiations are now exploited due to availability of commercial sources of terahertz radiations.

4.2.1 Application:

4.2.1.1 Pharmaceutical industry: tablet integrity and performance

Coating has a wide variety of functions. The most important function of coating is to regulate the controlled release of active ingredients in the body. Coating not only contributes to the bioavailability of a particular drug or combination of drugs during certain times and locations but also coating can protect the stomach from high concentrations of active ingredients, improve tablet visual appeal and extend shelf life by protecting the ingredients from degradation by moisture and oxygen. In relation to tablet coating the process analytical technology (PAT) initiative is intended to improve consistency and predictability of tablet action by improving quality and uniformity of tablet coatings. Issues with coating can arise from problems with the coating materials or flaws in the coating pan or spray process. If a coating is non-uniform or has surface defects then the desired dose delivery and bioavailability can be compromised. From this standpoint it is important to characterize tablet coating uniformity, both within a single tablet and across an entire batch to develop an understanding of the functional analysis of the final product. Several analytical and imaging techniques are being used to understand the critical processes involved in tablet coating but none of them is ideal to fully characterize the layers. Some of the techniques that provide useful information are atomic force microscopy, confocal laser microscopy, X-ray photoelectron spectroscopy, electron paramagnetic resonance, Fourier transform infrared spectroscopy, and laser induced breakdown spectroscopy (LIBS) and scanning thermal microscopy. However all these methods are either destructive to the tablet or cannot be readily implemented for rapid on-line measurement.

Terahertz image can be optimized for performing 3D analysis on tablets. It can enable to determine coating integrity and thickness, detect and identify localized chemical or physical structure such as cracks or chemical agglomeration within a core and to interrogate embedded layers (such as an interface between two layers) for delamination and integrity. Terahertz measurements may well become the primary method for the nondestructive determination of coating thickness, requiring little or no calibration for

most coatings and substrates. It can reveal the thickness, uniformity, distribution and coverage of simple and complex coating. Terahertz image can also detect embedded layers and localized chemical or physical structural features in the cores of intact tablets to confirm 3D morphology and blend uniformity.

4.2.1.2 Terahertz pulsed imaging (TPI)

TPI is a completely non-invasive and non-destructive pharmaceutical analysis tool using extremely low power, ultra short pulses of electromagnetic radiation at lower frequencies than infrared (1 THz = 1012 Hz). Terahertz spectroscopy has already proved useful to distinguish between different polymorph forms of the drug. TPI is a next step of this whereby THz pulses are used to image object of interest. THz pulses are generated by illuminating photoconductive semi-conductors with pulsed near-infrared laser radiation and detected coherently. Tablet coatings are semi-transparent to THz frequencies and do no scatter them significantly. THz pulses incident on a tablet surface penetrate through the different coating layers. At each interface a portion of THz radiations is reflected back to the detector. The amplitude of reflected THz radiation is recorded as a function of time. In this technique the sample itself is completely unaffected by the measurement. Coating thickness uniformity is established simply from the transit time of the pulse to each interface. With knowledge of the refractive index of coating material the actual thickness can be determined to a depth resolution of about 20 microns. The spot size of the THz pulse, and therefore lateral resolution, is about 250 microns.

4.2.1.3 Molecular structure

The sensitivity and specificity of terahertz spectroscopy to both intermolecular and intramolecular vibrations in different chemical species enable investigation of the crystalline state of drugs e.g. Polymorphism. The use of pulsed terahertz imaging in proteomics and drug discovery determines protein 3D structure, folding and characterization. It is also very sensitive to DNA hybridization and other interactions. Terahertz spectroscopy provides rapid identification of the different crystalline forms of

drug molecules – the polymorphs – which can exhibit different solubility's, stabilities and bioavailability and hence are an important factor in the therapeutic efficacy of a drug. Detecting and identifying the different polymorphs and understanding the mechanism and dynamics of polymorphic inter-conversion, is an important milestone in selecting the optimum form for further development and manufacture. It is possible not only to detect the differences between pure specimens of the polymorphs but terahertz spectroscopy can distinguish between specific polymorphic forms in tablet formulation.

Terahertz spectroscopy can also differentiate between different hydrate forms. Lactose which is one the most commonly used excipients in the pharmaceutical industry has at least three different hydrates namely α-monohydrate, α-anhydrate and β-anhydrate form. These three hydrate forms exhibit terahertz spectra that can be used for both quantitative and qualitative analysis. Terahertz region provides unique sensitivity to lattice structure enabling qualitative and qualitative analysis of crystalline and amorphous materials as well.

4.2.1.4 Time resolved THz spectroscopy of protein folding

Proteins fold, catalyze reactions, and transducer signals via binding to other biomolecules. These processes are driven by motions with characteristics time scales ranging from femtoseconds (fs) to milliseconds (ms). The characteristic modes from which such motions collectively emerge often cause large amplitude deformations of all or part of the protein. Temperature tuning reveals when certain modes are frozen out, while the terahertz spectroscopy can cover fast relaxation kinetics on fs time scale during which a protein rearranges its overall structure.

4.2.1.5 In dermatology

The cosmetic appearance of skin is directly linked to the outermost layer, the stratum corneum. The water content of the stratum corneum influences its permeability and elasticity. Most skin-care products such as moisturizers act to increase the retained

water content of this layer of the skin to enhance its appearance. Quantitative characterization of the hydration level of the stratum corneum is thus of crucial importance to the cosmetic industry in order to characterize and compare the effectiveness of their products.

Basal cell carcinoma (BCC) is the most common form of cancer worldwide in white populations and has a reported annual incidence of over 1 million in the U.S.A. Several different imaging techniques are being evaluated as diagnostic tools for skin lesions and tumor margin assessment. The terahertz (THz) frequency wavelength is of particular interest as it excites the intermolecular interactions, such as the librational and vibrational modes of molecules providing spectroscopic information. Terahertz pulse imaging (TPI) is a noninvasive, coherent optical imaging modality that explores this frequency region. These wavelengths are significantly larger than the scattering structures in tissue; therefore we assume that scattering effects are negligible. The current lateral and axial resolutions attainable with our system at 1 THz are 350 m and 40 m, respectively, making it a viable imaging modality. As TPI is a coherent, time gated, low noise technique, both phase and amplitude information can be obtained, from which the absorption and refractive index of a medium can be determined. This enables TPI to provide both structural and functional information, due to chemical specificity. Through examination of the terahertz waveform in both the time and frequency domains, TPI may prove advantageous in distinguishing type, lateral spread, and depth of tumors.

4.2.1.6 Oral healthcare

Dental carries or tooth decay is one of the most common human disorders. Carries proceed by the creation of a subsurface lesion in the enamel. The lesion may extend to the next tissue in the layer in teeth, the dentine, without macroscopically visible breakdown or even microcavity formation at the tooth surface. The absence of visual features on the tooth surface makes early detection of tooth decay difficult. X-rays which is one of the accepted methods used to detect decay, only reveals the problem at a relatively late stage, when drilling and filling is the only method available to halt the

decay. If decay can be detected early enough it is possible to reverse the process without the need for drilling by the use of either fissure sealing or remineralization.

Terahertz imaging can distinguish between the different types of tissue in a human tooth; detect carries at an early stage in the enamel layers of human teeth and monitor early erosion of the enamel at the surface of the tooth.

4.2.1.7 Oncology

It is estimated that more than 85% of all cancers originate in the epithelium. Excision biopsy to remove tissue from the body and examining it under a microscope is the gold standard for cancer diagnosis. Terahertz technology has the potential to greatly improve conventional biopsy and associated surgery by more precisely identifying the areas to be excised thereby reducing the number of procedures and facilitating earlier and more accurate diagnosis. As the technology develops, it may be possible to perform biopsies using live terahertz imaging of affected area, making possible point of care optical biopsy.

4.2.1.8 Detection of impurities in pharmaceutical industry

The manufacturing of pharmaceutical products is a highly monitored process that requires strict quality regulations. If the final product fails to meet the standard set by regulatory agencies then the whole batch is destroyed. This encourages the pharmaceutical industry to work on batch-processing techniques. Typically, pharmaceutical companies manufacture a finished product and then use laboratories to analyze a proportion of the batch to verify the quality of their product. Terahertz radiation has the ability to obtain information on chemical and physical structures and is able to accomplish this in real-time in a non-destructive form. This shows potential for the pharmaceutical industry as it is able to specifically determine the structure and properties of the sample to test, such as the bioavailability, manufacturability, purification, stability, dissolution rate, solubility and other performance characteristics of the drug. During manufacturing, solid pharmaceutical materials may come into contact with water or other impurities during processing, which can affect the product

performance. THz Spectroscopy can measure the unique physico-chemical properties of a product, being able to specifically distinguish one product from another which provides quality information. Terahertz Spectroscopy can also be used to patent pharmaceutical products because of the ability to distinguish the specific chemical components.

4.2.1.9 Medical imaging

Contrary to X-rays, terahertz radiation has relatively low photon energy for damaging tissues and DNA. Some frequencies of terahertz radiation can penetrate several millimeters of tissue with low water content (e.g., fatty tissue) and reflect back. Terahertz radiation can also detect differences in water content and density of a tissue. Such methods could allow effective detection of epithelial cancer with an imaging system that is safe, non-invasive, and painless.

Spectroscopy in terahertz radiation could provide novel information in chemistry and biochemistry. Recently developed methods of THz time-domain spectroscopy (THz TDS) and THz tomography have been shown to be able to perform measurements on, and obtain images of, samples that are opaque in the visible and near-infrared regions of the spectrum. The utility of THz-TDS is limited when the sample is very thin, or has a low absorbance, since it is very difficult to distinguish changes in the THz pulse caused by the sample from those caused by long-term fluctuations in the driving laser source or experiment. However, THz-TDS produces radiation that is both coherent and spectrally broad, so such images can contain far more information than a conventional image formed with a single-frequency source.

4.2.1.10 Security

Terahertz radiation can penetrate fabrics and plastics, so it can be used in surveillance, such as security screening, to uncover concealed weapons on a person, remotely. This is of particular interest because many materials of interest have unique spectral “fingerprints” in the terahertz range. This offers the possibility to combine spectral identification with imaging. Passive detection of terahertz signatures avoids the bodily

privacy concerns of other detection by being targeted to a very specific range of materials and objects.

At airports or other security critical places dangerous non-metallic substances like ceramic knifes or plastic explosives now can be detected with terahertz beams. This is possible because T-rays get through clothes, but cannot get through the upper skin (because of the water content).

4.2.1.11 Communication

Potential uses exist in high-altitude telecommunications, above altitudes where water vapor causes signal absorption: aircraft to satellite, or satellite to satellite.

CHAPTER 5

Platform: Comsol multiphysics version 4.2b

5.1 Creating a New Model

You can set up a model guided by the Model Wizard or start from a Blank Model.

5.1.2 CREATING A MODEL GUIDED BY THE MODEL WIZARD

The Model Wizard will guide you in setting up the space dimension, physics, and study type in a few steps:

1. Start by selecting the space dimension for your model component: 3D, 2D Axisymmetric, 2D, 1D Axisymmetric, or 0D.
2. Now, add one or more physics interfaces. These are organized in a number of Physics branches in order to make them easy to locate. These branches do not directly correspond to products. When products are added to your COMSOL Multiphysics installation, one or more branches will be populated with additional physics interfaces.
3. 3 Select the Study type that represents the solver or set of solvers that will be used for the computation. Finally, click Done. The desktop is now displayed with the model tree configured according to the choices you made in the Model Wizard.

5.1.3 CREATING A BLANK MODEL

The Blank Model option will open the COMSOL Desktop interface without any Component or Study. You can right-click the model tree to add a Component of a certain space dimension, physics interface, or Study.

5.2 PARAMETERS, VARIABLES, AND SCOPE

5.2.1 Global Parameters

Global parameters are user-defined constant scalars that are usable throughout the model. That is to say, they are “global” in nature. Important uses are:

• Parameterizing geometric dimensions.

• Specifying mesh element sizes.

• Defining parametric sweeps (simulations that are repeated for a variety of different values of a parameter such as a frequency or load).

A global parameter expression can contain numbers, global parameters, built-in constants, built-in functions with global parameter expressions as arguments, and unary and binary operators. For a list of available operators, Language Elements and Reserved Names”. Because these expressions are evaluated before a simulation begins, global parameters may not depend on the time variable t. Likewise, they may not depend on spatial variables like x, y, or z, nor on the dependent variables for which your equations are solving.It is important to know that the names of parameters are case sensitive.You define global parameters in the Parameters node in the model tree under Global Definitions.

5.2.2 Geometry

This tutorial uses a geometry that was previously created.

File Locations

The location of the application library that contains the file used in this exercise varies based on the software installation and operating system. In Windows, the file path will be similar to:

C:\Program Files\COMSOL\COMSOL52a\Multiphysics\applications.

1. In the Model Builder window, under Component 1, right-click Geometry 1 and select Import .As an alternative, you can use the ribbon and click Import from the Geometry tab.
2. In the Settings window for Import, from the Source list, select COMSOL Multiphysics file.
3. Click Browse and locate the file wrench. mphbin in the application library folder of the COMSOL installation folder. Its default location in Windows is:

C:\ProgramFiles\COMSOL\COMSOL52a\Multiphysics\applications\COMSOL_Multiphysics\ Structural_Mechanics\wrench.mphbin

Double-click to add or click Open.

5.2.3 Materials

The Materials node stores the material properties for all physics and all domains in a Component node. Use the same generic steel material for both the bolt and tool. Here is how to choose it in the Model Builder.

1. Open the Add Materials window. You can open the Add Materials window in either of these two ways:
   -Right-click Component 1 > Materials in the Model Builder and select Add Material
   - From the ribbon, select the Home tab and then click Add Material.
2. In the Add Material window, click to expand the Built-In folder. Scroll down to find Structural steel, right-click, and select Add to Component 1.
3. Examine the Material Contents section in the Settings window for Material to see the properties that are available. Properties with green check marks are used by the physics in the simulation.
4. Close the Add Material window.

5.3 SELECTING BOUNDARIES AND OTHER GEOMETRIC ENTITIES

When a boundary is unselected, its color is typically gray, the exception being when you use the material Appearance setting available in Materials; To select a boundary, first hover over it. This highlights the boundary in red, assuming the boundary was previously unselected. Now, click to select the boundary by using the left mouse button. The boundary now turns blue. Its boundary number will appear in the Selection list in the Settings window of the corresponding boundary condition. Once a boundary is selected and you hover over it again, the boundary turns green. If you click a boundary highlighted in green, the boundary is deselected and now turns gray again. The same technique for selecting and deselecting is applicable to geometry objects, domains, boundaries, edges, and points.

5.3.1 Mesh

The mesh settings determine the resolution of the finite element mesh used to discretize the model. The finite element method divides the model into small elements of geometrically simple shapes, in this case tetrahedrons. In each tetrahedron, a set of polynomial functions is used to approximate the structural displacement field — how much the object deforms in each of the three coordinate directions.

In this example, because the geometry contains small edges and faces, you will define a slightly finer mesh than the default setting suggests. This will better resolve the variations of the stress field and give a more accurate result. Refining the mesh size to improve computational accuracy always involves some sacrifice in speed and typically requires increased memory usage.

5.3.2 Study

In the beginning of setting up the model, you selected a Stationary study, which implies that a stationary solver will be used. For this to be applicable, the assumption is that the load, deformation, and stress do not vary in time. To start the solver:

- Right-click Study 1 and select Compute (or press F8).After a few seconds of computation time, the default plot is displayed in the Graphics window. You can find other useful information about the computation in the Messages and Log windows; Click the Messages and Log tabs under the Graphics window to see the kind of information available to you. The Messages window can also be opened from the Windows drop-down list in the Home tab of the ribbon.

5.3.3 Results:

The von Mises stress is displayed in the Graphics window in a default Surface plot with the displacement visualized using a Deformation subnode. Change the default unit (N/m2) to the more suitable MPa as shown in the following steps.

CHAPTER 6
Background Material

At TOPAS Advanced Polymers, we deliver advanced plastic materials that enable product designers and manufacturers to take a step beyond the ordinary. Our TOPAS® COC resins are a chemical relative of polyethylene and other polyolefin plastics. But they offer a lot more. TOPAS cyclic olefin copolymers are ultra-pure, crystal-clear materials with a wide range of unique properties that enable our customers to surpass the competition.

Key properties and uses of TOPAS COC resin grades include:

- **Purity**: from direct drug contact to food packaging films, TOPAS COC medical plastics have very broad global regulatory approval
- **Glass-Clear**: lightweight optics, sparkling films, glass-like healthcare containers, and high performance diagnostics with UV transparency
- **Amorphous**: heat resistance in PCR plates, packaging, sterilizable devices and more, plus thermo formability
- **Olefin**: compatible blends with polyethylene, often with improved reclaim and recycle characteristics for sustainability
- **Barrier**: resists moisture, alcohols, acids and more for product protection in foods, medicine, and electronics

COC exhibits a unique combination of properties, which can be customized by varying the chemical structure of the copolymer. Performance benefits include:

- Low density
- High transparency
- Low birefringence
- Extremely low water absorption
- Excellent water vapor barrier properties
- Adjustable heat deflection temperature up to 170 °C
- High rigidity, strength and hardness
- Excellent biocompatibility
- Very good melt processability/flowability
- High resistance to acids and alkalis
- Very good electrical insulating properties

CHAPTER 7

FACTORS AND LOSSES IN OPTICAL FIBER

7.1 SINGLE MODE FIBER

In fiber-optic communication, a **single-mode optical fiber** (**SMF**) is an optical fiber designed to carry light only directly down the fiber - the transverse mode. Modes are the possible solutions of the Helmholtz equation for waves, which is obtained by combining Maxwell's equations and the boundary conditions. These modes define the way the wave travels through space, i.e. how the wave is distributed in space. Waves can have the same mode but have different frequencies. This is the case in single-mode fibers, where we can have waves with different frequencies, but of the same mode, which means that they are distributed in space in the same way, and that gives us a single ray of light. Although the ray travels parallel to the length of the fiber, it is often called transverse mode since its electromagnetic vibrations occur perpendicular (transverse) to the length of the fiber. The 2009 Nobel Prize in Physics was awarded to Charles K. Kao for his theoretical work on the single-mode optical fiber.

7.1.1 Characteristics:

Like multi-mode optical fibers, single mode fibers do exhibit modal dispersion resulting from multiple spatial modes but with narrower modal dispersion. Single mode fibers are therefore better at retaining the fidelity of each light pulse over longer distances than multi-mode fibers. For these reasons, single-mode fibers can have a higher bandwidth than multi-mode fibers. Equipment for single mode fiber is more expensive than equipment for multi-mode optical fiber, but the single mode fiber itself is usually cheaper in bulk.

A typical single mode optical fiber has a core diameter between 8 and 10.5 μm and a cladding diameter of 125 μm. There are a number of special types of single-mode

optical fiber which have been chemically or physically altered to give special properties, such as dispersion-shifted fiber and nonzero dispersion-shifted fiber. Data rates are limited by polarization mode dispersion and chromatic dispersion. As of 2005, data rates of up to 10 gigabits per second were possible at distances of over 80 km (50 mi) with commercially available transceivers (Xenpak). By using optical amplifiers and dispersion-compensating devices, state-of-the-art DWDM optical systems can span thousands of kilometers at 10 Gbit/s, and several hundred kilometers at 40 Gbit/s.

The lowest-order bounds mode is ascertained for the wavelength of interest by solving Maxwell's equations for the boundary conditions imposed by the fiber, which are determined by the core diameter and the refractive indices of the core and cladding. The solution of Maxwell's equations for the lowest order bound mode will permit a pair of orthogonally polarized fields in the fiber, and this is the usual case in a communication fiber.

In step-index guides, single-mode operation occurs when the normalized frequency, *V*, is less than or equal to 2.405. In practice, the orthogonal polarizations may not be associated with degenerate modes.

$$V = \frac{2\pi r f}{c}\sqrt{{n_{co}}^2 - {n_{cl}}^2} \leq 2.405,$$

OS1 and OS2 are standard single-mode optical fiber used with wavelengths 1310 nm and 1550 nm (size 9/125 µm) with a maximum attenuation of 1 dB/km (OS1) and 0.4 dB/km(OS2). OS1 is defined in ISO/IEC 11801,[7] and OS2 is defined in ISO/IEC 24702.

7.2 MULTI MODE FIBER

Multi-mode optical fiber is a type of optical fiber mostly used for communication over short distances, such as within a building or on a campus. Typical multimode links have data rates of 10 Mbit/s to 10 Gbit/s over link lengths of up to 600 meters (2000 feet).

7.2.1 Applications

The equipment used for communications over multi-mode optical fiber is less expensive than that for single-mode optical fiber. Typical transmission speed and distance limits are 100 Mbit/s for distances up to 2 km (100BASE-FX), 1 Gbit/s up to 1000 m, and 10 Gbit/s up to 550 m.

Because of its high capacity and reliability, multi-mode optical fiber generally is used for backbone applications in buildings. An increasing number of users are taking the benefits of fiber closer to the user by running fiber to the desktop or to the zone. Standards-compliant architectures such as Centralized Cabling and fiber to the telecom enclosure offer users the ability to leverage the distance capabilities of fiber by centralizing electronics in telecommunications rooms, rather than having active electronics on each floor.

7.2.2 Comparison with single-mode fiber

The main difference between multi-mode and single-mode optical fiber is that the former has much larger core diameter, typically 50–100 micrometers; much larger than the wavelength of the light carried in it. Because of the large core and also the possibility of large numerical aperture, multi-mode fiber has higher "light-gathering" capacity than single-mode fiber. In practical terms, the larger core size simplifies connections and also allows the use of lower-cost electronics such as light-emitting diodes (LEDs) and

vertical-cavity surface-emitting lasers (VCSELs) which operate at the 850 nm and 1300 nm wavelength (single-mode fibers used in telecommunications typically operate at 1310 or 1550 nm). However, compared to single-mode fibers, the multi-mode fiber bandwidth–distance product limit is lower. Because multi-mode fiber has a larger core-size than single-mode fiber, it supports more than one propagation mode; hence it is limited by modal dispersion, while single mode is not.

The LED light sources sometimes used with multi-mode fiber produce a range of wavelengths and these each propagate at different speeds. This chromatic dispersion is another limit to the useful length for multi-mode fiber optic cable. In contrast, the lasers used to drive single-mode fibers produce coherent light of a single wavelength. Due to the modal dispersion, multi-mode fiber has higher pulse spreading rates than single mode fiber, limiting multi-mode fiber's information transmission capacity.

Single-mode fibers are often used in high-precision scientific research because restricting the light to only one propagation mode allows it to be focused to an intense, diffraction-limited spot.

Jacket color is sometimes used to distinguish multi-mode cables from single-mode ones. The standard TIA-598C recommends, for non-military applications, the use of a yellow jacket for single-mode fiber, and orange or aqua for multi-mode fiber, depending on type. Some vendors use violet to distinguish higher performance OM4 communications fiber from other types.

7.3 Material Absorption loss

Absorption of signal is a serious loss mechanism in an optical fiber. Absorption occurs in optical fibers due to the presence of imperfections in the atomic structure of the fiber material, due to some basic inherent intrinsic material properties and due to some extrinsic material properties. Imperfections may appear in atomic structure due to oxygen deficiencies and missing of certain molecules. Diffusion of hydrogen molecules may also induce absorption. But the contribution from imperfections is relatively small in fiber optic absorption losses. Inherent intrinsic absorption is caused by basic fiber material properties. If a material is free from impurities and imperfections, then entire absorption is due to intrinsic absorption. Silica fibers possess very low intrinsic material absorption. Here absorption is caused by the vibration of silicon-oxygen bonds. The interaction between these bonds and the electromagnetic field of the optical signal is responsible for intrinsic absorption. Presence of impurities in the fiber material leads to extrinsic absorption. This is caused by the electronic transition of metal impurity ions from one energy level to another. Another reason for extrinsic absorption is the presence of hydroxyl ions in the fiber.

$$\alpha_{eff} = \sqrt{\frac{\varepsilon_0}{\mu_0}}\left(\frac{\int_{mat} n_{mat}|E|^2\alpha_{mat}\,dA}{\left|\int_{all} S_z\,dA\right|}\right)$$

Where, ε_0 and μ_0 are considered to be the relative permittivity and permeability in vacuum respectively, n_{mat} is the refractive index of Topas, α_{mat} is the bulk material absorption loss, $\boldsymbol{E}$ is the modal electric field and S_z is the z component of the pointing vector (S_z = ½($\mathbf{E} \times \mathbf{H}^*$).z), where **E** and **H** are the electric and magnetic fields respectively.Fig.5 depicts the characteristics of EML as a function of core diameter with different core porosities. From where it is observed that, for the same porosity values there is a significant change of EML when the core diameter changes.

It is a loss mechanism related to the material composition and fabrication process of the fiber which results in the dissipation of some of the transmitted optical power as heat in

waveguide. The absorption of light may be intrinsic (caused by one or more major components of glass) or extrinsic (caused by impurities within the glass).

7.4 Mode Power propagation

The amount of useful power propagating through different regions of the fiber also known as core power fraction can be calculated by,

$$\eta' = \frac{\int_X S_z dA}{\int_{all} S_z dA}$$

Where η' represents mode power fractionand X represents the area of interests. To design a standard PCF, it is necessary to pass most of the useful power through the core air holes. Higher D_{core} increases the core power fraction but this also increases the EML. On the other hand, as the D_{core} decreases EML also decreases but this also decreases the core power fraction. These are contradictory conditions and needs to select an optimum condition of higher core power fraction and lower EML. At different core porosities, the characteristics of core power fraction as a function of core diameter where it can be observed that amount of core power increases with the increase of core diameter.

7.5 Confinement Loss

PCFs are a new class of optical fibers, which has concerned fabulous attention in the last few years. PCFs are normally formed with silica having air holes positioned in the cladding region. PCFs have novel properties because the effective refractive index has burly wavelength dependence and huge design flexibility. PCFs main applications range from telecommunication field to metrology, spectroscopy, microscopy, medical diagnostics equipment, biology and sensing. There are several parameters to manipulate: pitch, air hole shape and diameter, refractive index of the glass, and type of lattice. PCFs structures can have hexagonal lattice or octagonal lattice or square lattice.

By changing the lattices and lattice parameters like pitch, air hole diameter and changing rings in the cladding region, the properties of PCFs can also be changed.

Many experiments and investigations have been carried out using different analysis techniques and tools to understand the propagation properties of various PCFs. PCFs also known as micro-structured or holey fibers are made of the refractive index periodicity, with the arrangement of air holes around the core. Many rings around the core help to ensnare light well within the core minimizing the confinement loss. Based on structure, PCFs can be either solid core high-index guiding fibers or hollow core low index guiding fibers. The index guiding PCFs guide light in a solid core by modified total internal reflection (M-TIR) like to the conventional optical fibers. Hollow core PCFs guide light by the photonic band gap (PBG) effect. Light is confined in the low-index core, as the distribution of energy levels in the structure makes the propagation in the cladding region impossible. In both cases, to attain the lowest amount loss, air holes should be continual to infinity which is unfeasible. So, modes leak in cladding and confinement loss is created. The confinement loss can be reduced by proper design of structure parameters in PCFs, and consequently, mode leakage to cladding is avoided. Already, many reports have been published about PCFs with low confinement loss. At 0.8 μm center wavelength the confinement loss is found 10-8 dB/m, 10-6 dB/m and 10-4 dB/m for 2 μm, 1.8 μm and 1.6 μm lattice pitches. Again at 1.55 μm center wavelength for three rings hexagonal PCFs the confinement loss is 10-3 dB/km but Ademgil and Huxha obtained this loss which was varied from 10-1to 10-5 dB/m [10]. Also at 1.3 μm center wavelength this confinement loss was found 10-8 dB/km for circular ring PCFs.

Another important parameter to be considered for PCF design is confinement loss. It depends upon the core porosity and the number of air holes used in cladding. It can be calculated by taking the imaginary part of the complex refractive index. The confinement loss can be calculated by,

$$L_C = 8.686\ (\frac{2\pi f}{c})\mathrm{Im}(n_{eff})(\ ^{dB}/_{m}\ ),$$

where, *f* is the frequency of the guiding light, *c* is speed of light in vacuum and Im (n_{eff}) symbolizes the imaginary part of the refractive index. The confinement loss as a

function of frequency where it is observed that as the frequency increases, the confinement loss scaled down.

7.6 Dispersion

In optics, dispersion is the phenomenon in which the phase velocity of a wave depends on its frequency. Media having this common property may be termed dispersive media. Sometimes the term chromatic dispersion is used for specificity. Although the term is used in the field of optics to describe light and other electromagnetic waves, dispersion in the same sense can apply to any sort of wave motion such as acoustic dispersion in the case of sound and seismic waves, in gravity waves (ocean waves), and for telecommunication signals propagating along transmission lines (such as coaxial cable) or optical fiber.

In optics, one important and familiar consequence of dispersion is the change in the angle of refraction of different colors of light, as seen in the spectrum produced by a dispersive prism and in chromatic aberration of lenses. Design of compound achromatic lenses, in which chromatic aberration is largely cancelled, uses a quantification of a glass's dispersion given by its Abbe number V, where lower Abbe numbers correspond to greater dispersion over the visible spectrum. In some applications such as telecommunications, the absolute phase of a wave is often not important but only the propagation of wave packets or "pulses"; in that case one is interested only in variations of group velocity with frequency, so-called group-velocity dispersion (GVD).

7.6.1 Material and waveguide dispersion

Most often, chromatic dispersion refers to bulk material dispersion, that is, the change in refractive index with optical frequency. However, in a waveguide there is also the phenomenon of waveguide dispersion, in which case a wave's phase velocity in a structure depends on its frequency simply due to the structure's geometry. More generally, "waveguide" dispersion can occur for waves propagating through any

inhomogeneous structure (e.g., a photonic crystal), whether or not the waves are confined to some region. In a waveguide, both types of dispersion will generally be present, although they are not strictly additive. For example, in fiber optics the material and waveguide dispersion can effectively cancel each other out to produce a Zero-dispersion wavelength, important for fast Fiber-optic communication.

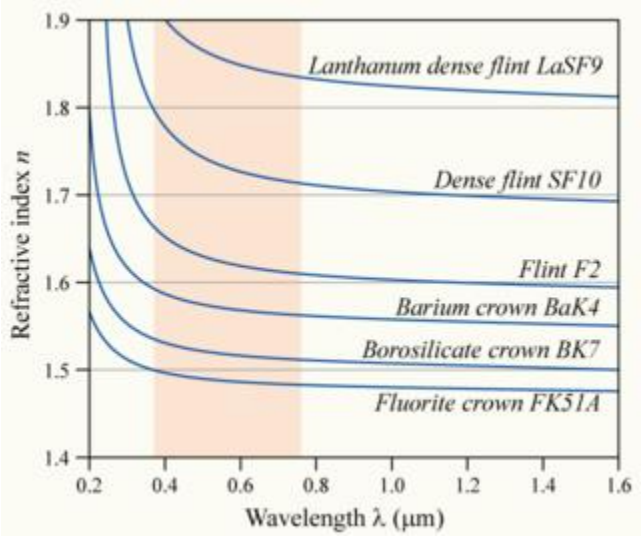

Fig 7.1 Material dispersion in optics

The variation of refractive index vs. vacuum wavelength for various glasses. The wavelengths of visible light are shaded in red.

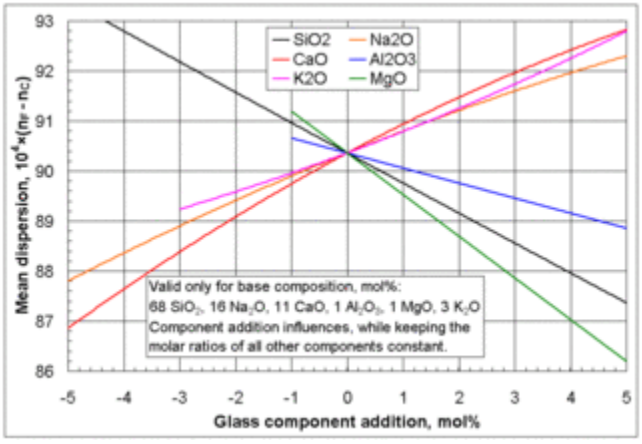

Fig 7.2 Mean dispersion in terms of mole

Influences of selected glass component additions on the mean dispersion of a specific base glass (n_F valid for $\lambda = 486$ nm (blue), n_C valid for $\lambda = 656$ nm (red).

Material dispersion can be a desirable or undesirable effect in optical applications. The dispersion of light by glass prisms is used to construct spectrometers and spectro radiometers. Holographic gratings are also used, as they allow more accurate discrimination of wavelengths. However, in lenses, dispersion causes chromatic aberration, an undesired effect that may degrade images in microscopes, telescopes and photographic objectives.

In general, the refractive index is some function of the frequency f of the light, thus $n = n(f)$, or alternatively, with respect to the wave's wavelength $n = n(\lambda)$. The wavelength dependence of a material's refractive index is usually quantified by its Abbe number or its coefficients in an empirical formula such as the Cauchy or Sellmeier equations.

Because of the Kramers–Kronig relations, the wavelength dependence of the real part of the refractive index is related to the material absorption, described by the imaginary part of the refractive index (also called the extinction coefficient). In particular, for non-magnetic materials ($\mu = \mu_0$), the susceptibility χ that appears in the Kramers–Kronig relations is the electric susceptibility $\chi_e = n^2 - 1$.

The most commonly seen consequence of dispersion in optics is the separation of white light into a color spectrum by a prism. From Snell's law it can be seen that the angle of refraction of light in a prism depends on the refractive index of the prism material. Since that refractive index varies with wavelength, it follows that the angle that the light is refracted by will also vary with wavelength, causing an angular separation of the colors known as angular dispersion.

In this case, the medium is said to have normal dispersion. Whereas, if the index increases with increasing wavelength (which is typically the case for X-rays, the medium is said to have anomalous dispersion.

At the interface of such a material with air or vacuum (index of ~1), Snell's law predicts that light incident at an angle θ to the normal will be refracted at an angle arcsin(sin θ/n). Thus, blue light, with a higher refractive index, will be bent more strongly than red light, resulting in the well-known rainbow pattern.

7.6.2 Group Velocity Dispersion

Another consequence of dispersion manifests itself as a temporal effect. The formula v = c/n calculates the phase velocity of a wave; this is the velocity at which the phase of any one frequency component of the wave will propagate. This is not the same as the group velocity of the wave, that is the rate at which changes in amplitude (known as the envelope of the wave) will propagate. For a homogeneous medium, the group velocity v_g is related to the phase velocity v by (here λ is the wavelength in vacuum, not in the medium):

The group velocity v_g is often thought of as the velocity at which energy or information is conveyed along the wave. In most cases this is true, and the group velocity can be thought of as the signal velocity of the waveform. In some unusual circumstances, called cases of anomalous dispersion, the rate of change of the index of refraction with respect to the wavelength changes sign (becoming negative), in which case it is possible for the group velocity to exceed the speed of light ($v_g > c$). Anomalous dispersion occurs, for instance, where the wavelength of the light is close to an absorption resonance of the medium. When the dispersion is anomalous, however, group velocity is no longer an indicator of signal velocity. Instead, a signal travels at the speed of the wavefront, which is c irrespective of the index of refraction. Recently, it has become possible to create gases in which the group velocity is not only larger than the speed of light, but even negative. In these cases, a pulse can appear to exit a medium before it enters. Even in these cases, however, a signal travels at, or less than, the speed of light, as demonstrated by Stenner, et al.

The group velocity itself is usually a function of the wave's frequency. This results in group velocity dispersion (GVD), which causes a short pulse of light to spread in time as

a result of different frequency components of the pulse travelling at different velocities. GVD is often quantified as the group delay dispersion parameter (again, this formula is for a uniform medium only).

If D is less than zero, the medium is said to have positive dispersion. If D is greater than zero, the medium has negative dispersion. If a light pulse is propagated through a normally dispersive medium, the result is the higher frequency components travel slower than the lower frequency components. The pulse therefore becomes positively chirped, or up-chirped, increasing in frequency with time. Conversely, if a pulse travels through an anomalously dispersive medium, high frequency components travel faster than the lower ones, and the pulse becomes negatively chirped, or down-chirped, decreasing in frequency with time.

The result of GVD, whether negative or positive, is ultimately temporal spreading of the pulse. This makes dispersion management extremely important in optical communications systems based on optical fiber, since if dispersion is too high, a group of pulses representing a bit-stream will spread in time and merge, rendering the bit-stream unintelligible. This limits the length of fiber that a signal can be sent down without regeneration. One possible answer to this problem is to send signals down the optical fibre at a wavelength where the GVD is zero (e.g., around 1.3–1.5 μm in silica fibres), so pulses at this wavelength suffer minimal spreading from dispersion. In practice, however, this approach causes more problems than it solves because zero GVD unacceptably amplifies other nonlinear effects (such as four wave mixing). Another possible option is to use soliton pulses in the regime of anomalous dispersion, a form of optical pulse which uses a nonlinear optical effect to self-maintain its shape. Solitons have the practical problem, however, that they require a certain power level to be maintained in the pulse for the nonlinear effect to be of the correct strength. Instead, the solution that is currently used in practice is to perform dispersion compensation, typically by matching the fiber with another fiber of opposite-sign dispersion so that the dispersion effects cancel; such compensation is ultimately limited by nonlinear effects such as self-phase modulation, which interact with dispersion to make it very difficult to undo.

Dispersion control is also important in lasers that produce short pulses. The overall dispersion of the optical resonator is a major factor in determining the duration of the pulses emitted by the laser. A pair of prisms can be arranged to produce net negative dispersion, which can be used to balance the usually positive dispersion of the laser medium. Diffraction gratings can also be used to produce dispersive effects; these are often used in high-power laser amplifier systems. Recently, an alternative to prisms and gratings has been developed: chirped mirrors. These dielectric mirrors are coated so that different wavelengths have different penetration lengths, and therefore different group delays. The coating layers can be tailored to achieve a net negative dispersion.

7.6.3 Dispersion in waveguides

Waveguides are highly dispersive due to their geometry (rather than just to their material composition). Optical fibers are a sort of waveguide for optical frequencies (light) widely used in modern telecommunications systems. The rate at which data can be transported on a single fiber is limited by pulse broadening due to chromatic dispersion among other phenomena.

In general, for a waveguide mode with an angular frequency ω(β) at a propagation constant β (so that the electromagnetic fields in the propagation direction z oscillate proportional to $e^{i(\beta z-\omega t)}$), the group-velocity dispersion parameter D is defined as:

$$\beta_2 = \frac{2}{c}\frac{dn_{eff}}{d\omega} + \frac{\omega}{c}\frac{d^2 n_{eff}}{d\omega^2}$$

Where λ = 2πc/ω is the vacuum wavelength and v_g = dω/dβ is the group velocity. This formula generalizes the one in the previous section for homogeneous media, and

includes both waveguide dispersion and material dispersion. The reason for defining the dispersion in this way is that |D| is the (asymptotic) temporal pulse spreading Δt per unit bandwidth Δλ per unit distance travelled, commonly reported in ps / nm km for optical fibers.

In the case of multi-mode optical fibers, so-called modal dispersion will also lead to pulse broadening. Even in single-mode fibers, pulse broadening can occur as a result of polarization mode dispersion (since there are still two polarization modes). These are not examples of chromatic dispersion as they are not dependent on the wavelength or bandwidth of the pulses propagated.

7.7 Effective Area:

The effective area (A_{eff}) of the proposed fiber is also discussed, which can be calculated by [33]

$$A_{eff} = \frac{[\int I(r)rdr]^2}{\left[\int I^2(r)dr\right]^2},$$

Where; $I(r) = |E_t|^2$ is defined as the transverse electric field intensity distribution in the cross section of the fiber. The A_{eff} as a function of frequency, from where it is observed that as the frequency increases from 0.9 THz the A_{eff} decreases. It is because of more light spread for f>1 THz.It is also observed that at operating parameters, the calculated A_{eff} is very much comparable.

CHAPTER 8

Designs

We have used COMSOL Multi-Physics 4.3b for our designing. It can be interface with MATLAB for programming & plotting.

Before showing our implemented designs, we would like to introduce some important parameters which act as tremendous factor for designing a fiber are described below.

8.1 Parameters

Table 8.1: Parameter defination

Parameter	Parameter definition	Value
AFF	Air Filling fraction	Depends on design
D	Core Diameter	Depends on design
A	Distance between two adjacent air holes in the cladding	D/(2-AFF)
d	Cladding Air hole Diameter	AFF*A
F	Frequency	1 [THz]
Porosity	Ratio of the cross sectional area of air holes in the core to total cross sectional area of the core	Depends on design
Ac	Distance between two adjacent air holes in the core	Related to A
K	Proportionality Constant	sqrt(porosity*D^2/(n1*Ac^2))
n1	Number of holes in the core	Depends on design
rc	Radius of each air holes in the core	k*Ac/2

8.1.1 Air Filling Fraction

The diameter of air-holes in the cladding is d, and the pitch is A. AFF is defined as the ratio of diameter of air holes in the cladding to the pitch of the cladding.

The spacing between air holes lying on the same ring in the cladding is Λ1, which is related to Λ. The spacing between air-holes on the adjacent ring of the porous core is Λ_C and is related to Λ. The diameter of the air holes in cladding region was denoted as d and the air filling fraction (AFF) d/Λ has to be fixed throughout the whole numerical analysis because such higher air filling fraction increases the core confinement and reduce the Effective Material Loss (EML).This value of this AFF in the cladding cannot be increased further because further extension will cause overlapping the air holes and in that case the fabrication will be difficult.

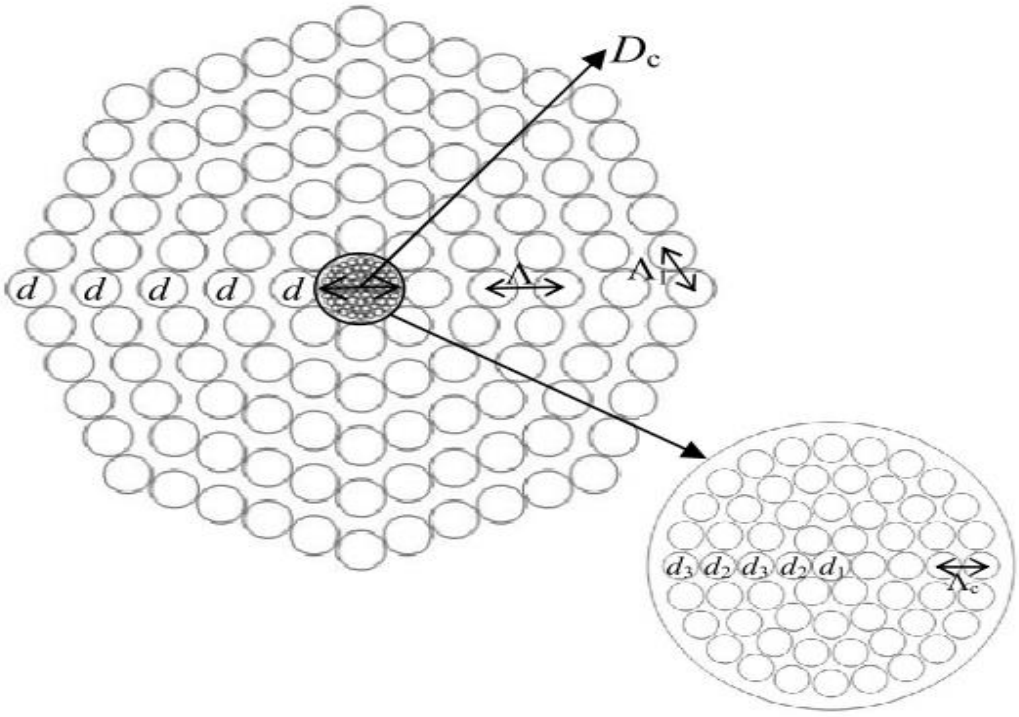

Fig 8.1: Transverse cross-section of five rings PC-OPCF

8.1.2 Porosity

The air hole size of the core determines the porosity which is defined as the ratio of the air hole area to the cross-section area of the core.

8.2 Designing Rules

The increasing number of rings in the cladding increases the confinement properties of the material which also reduces the material absorption loss.

Since the air holes in the core operate as a low index discontinuities and dry air is transparent in THz frequency band and for this reason the material absorption loss can be considerably reduced. The core of our implemented fibers is designed in such a way that the guiding mechanism is based on total internal reflection.

In the meantime, the AFF in the core diameter D_{core} =2(Λ-d/2) is variable and mostly determined by the core porosity. Porosity, frequency and core diameter is varied throughout the analytical process but at the same time the single mode condition is checked.

For all the simulations, five rings of air holes were used for cladding and three rings of air holes have been used for cores.

8.3 Our Implemented Designs

- ✓ Decagonal Cladding and Octagonal Core
- ✓ Octagonal Cladding and Rectangular core
- ✓ Hexagonal Cladding and Hexagonal Core
- ✓ Decagonal Cladding and Rotate Hexagonal Core
- ✓ Hexagonal Cladding and Spider Core

8.3.1 Decagonal Cladding and Octagonal Core

The air holes in the core are arranged in a octagonal and the cladding are arranged in decagonal structure.

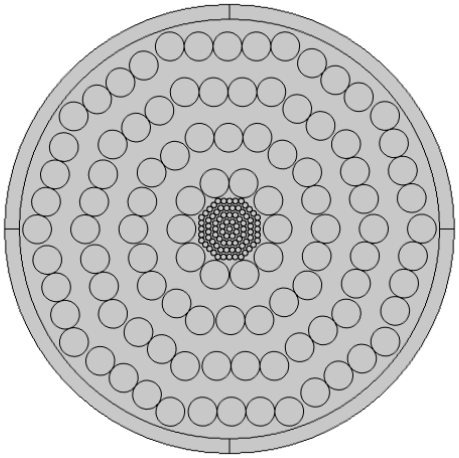

Fig 8.2: Decagonal Cladding and Octagonal Core

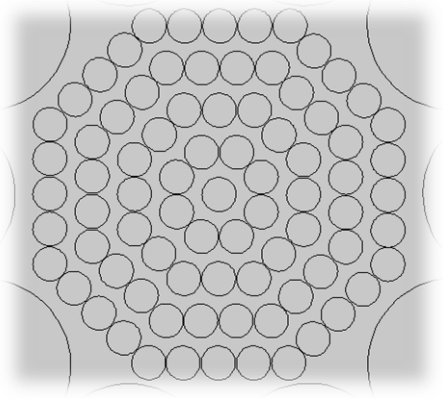

Fig 8.3: octagonal core

8.3.1.1 Obtained Results:

Factors	Values
EML (Effective Material loss)	0.17593 cm^{-1}
Mode Power propagation	18%

8.3.2 Octagonal Cladding and Rectangular core

The air holes in the core are arranged in a rectangular and the cladding are arranged in octagonal structure.

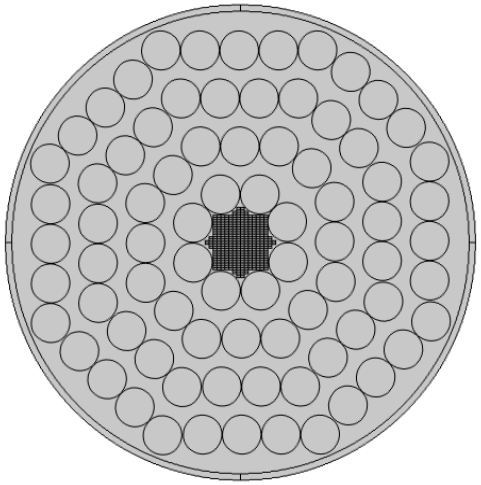

Fig 8.4: Octagonal Cladding and Rectangular core

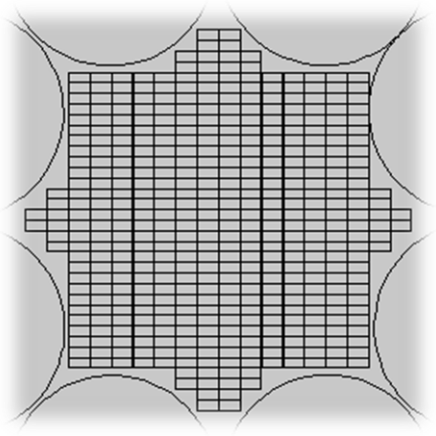

Fig 8.5: Rectangular core

8.3.2.1 Obtained Results:

Factors	Values
EML (Effective Material loss)	0.11652 cm^{-1}
Mode Power propagation	27%

8.3.3 Decagonal Cladding and Rotate Hexagonal Core

The air holes in the core are arranged in a rotate hexagonal and the cladding are arranged in decagonal structure.

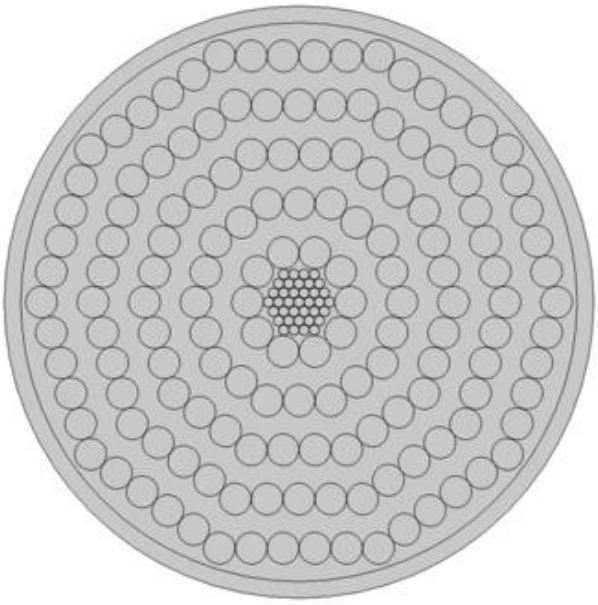

Fig 8.6: Decagonal Cladding and Rotate Hexagonal Core

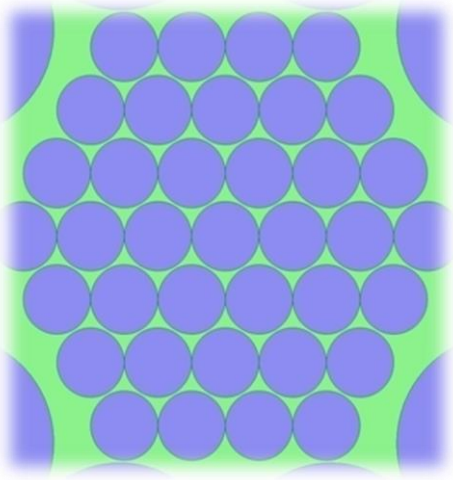

Fig 8.7: Rotate hexa core

8.3.3.1 Obtained Results:

Factors	Values
EML (Effective Material loss)	0.0492 cm^{-1}
Mode Power propagation	43%

8.3.4 Hexagonal Cladding and Spider Core

The air holes in the core are arranged in a spider and the cladding are arranged in hexagonal structure.

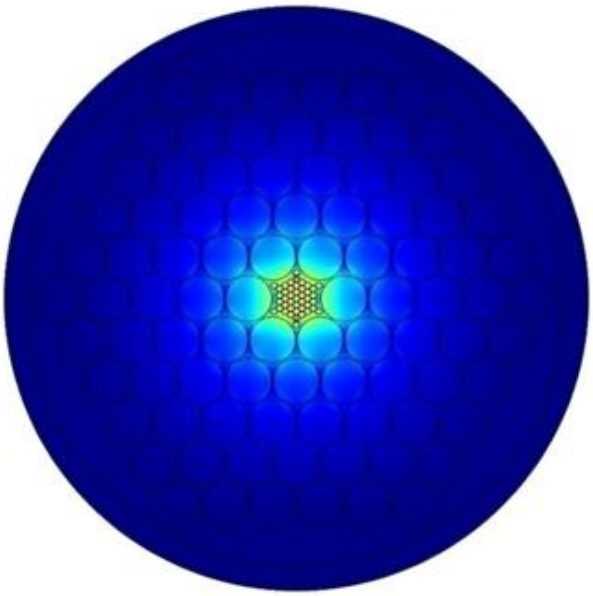

Fig 8.8: Hexagonal Cladding and Spider Core

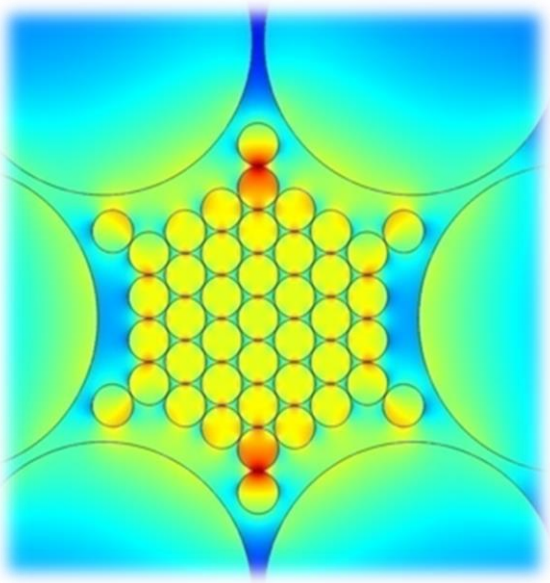

Fig 8.9: spider core

8.3.4.1 Obtained Results:

Factors	Values
EML (Effective Material loss)	0.04072 cm^{-1}
Mode Power propagation	15%

CHAPTER 9

OUR PROPOSED DESIGN

9.1 Overview

To make the guided Transmission more efficient & reliable in case of THz wave, a porous core rotate hexagonal crystal fiber with decagonal cladding structure is presented with theoretical & simulation result in this paper. This combination of core & cladding is absolutely new in the word of designing of optical fiber. The finite element method (FEM) with perfectly matched layer is used to investigate transmission characteristics. The proposed design gives an exceedingly low material loss of 0.0492cm^{-1}with a high power fraction of 43% for an operating frequency of 1 THz. Importance was also given to confinement loss & dispersion & thus they are analyzed & demonstrated. In addition, core diameter, porosity & fabrication procedure are also reported.

In this paper, a porous-core with rotate hexagonal structure & decagonal PCF in the cladding is proposed to significantly reduce the material loss. In this design, a larger air filling fraction (AFF) is used &TOPAS is used as the background material which together made it possible to give an effective material loss of 0.0492 cm^{-1} for a core diameter of 280μm with an operating frequency of 1 THz. The design also gives a higher power fraction 43%.

9.2 Main Design & Methodology

The arrangement of air holes in the cladding is in decagonal and the air holes in the core are in rotate hexagonal structure. Decagonal structure for the cladding is chosen because of its better confinement.

The term porosity which depends on the air hole size of the core is defined as the ratio of the air hole area to the cross section area of the core. . If porosity is reduced, then most of the power will be spread into cladding. As the air holes in the core perform as a low index material and dry air [α_{mat}=0] is transparent in the THz frequency range, the absorption loss of material can be significantly decreased. The proposed design of the core is based on the total internal reflection at the core.

The cross section of the proposed design which is decagonal structure in the cladding & hexagonal in the core with an enlarged version of the core is shown in fig 1 and the power flow distribution is shown in fig 2.

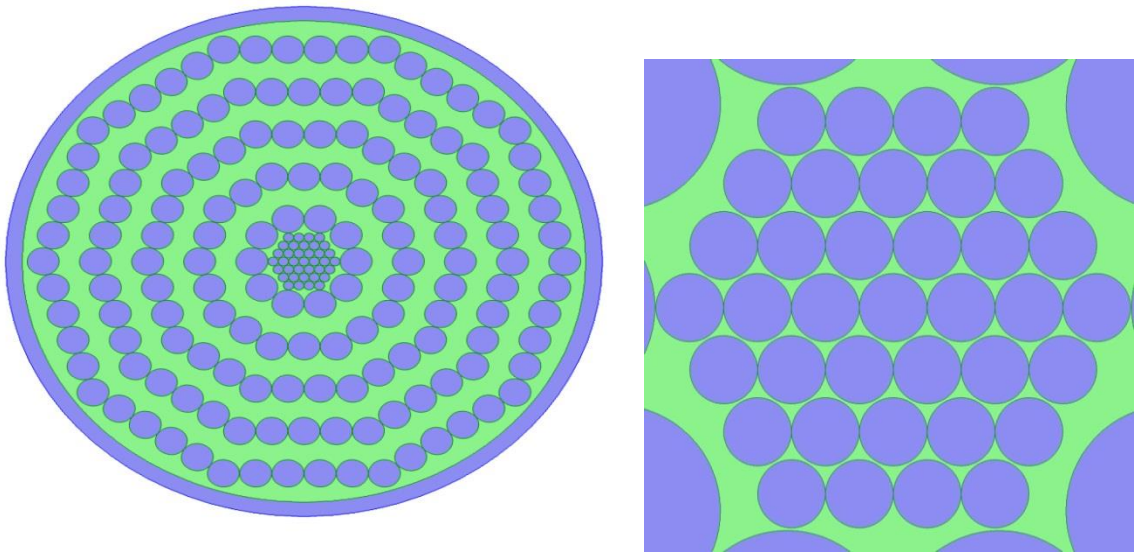

(a) (b)

Fig 9.1: Cross section of the (a) proposed photonic crystal fiber & (b) enlarge version of porous core

The distance between two adjacent air holes on the same ring in the cladding is A_1 that is related to A by A_1 =0.766*A. The distance between air holes on the adjacent ring of the porous core is A_c which is related to A by A_c= 0.245*A.

The core diameter, D_{core} =2(A-d/2) has been changed while the air filling fraction (AFF) d/A was preserved fixed at 0.76 throughout the whole design where d is the diameter of the air holes in cladding region and A is the outer pitch(distance between two adjacent air holes of the cladding region). Such higher AFF increases the core confinement and reduces the effective material loss (EML). AFF can't be increased further because it causes overlapping the air holes in the cladding and hence fabrication will be challenging.

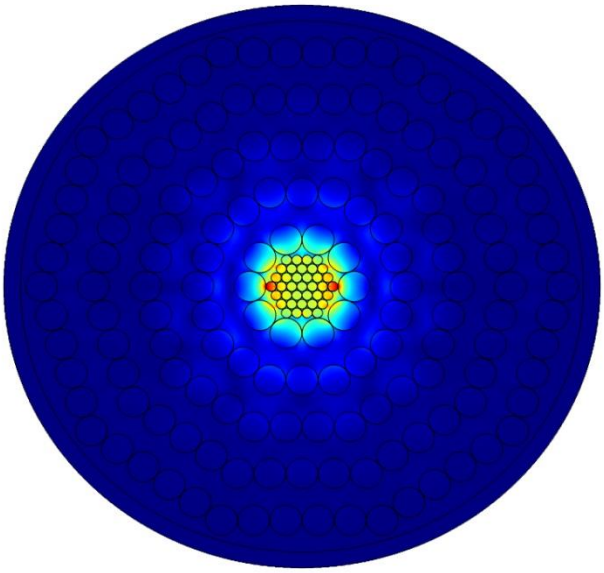

Fig 9.2: Power flow distribution of the proposed PCF

For all the simulation, five rings of air holes in cladding and threerings of air holes in the core is used so that more of the light is passed through the core & thus confinement is gained.

In the proposed design, TOPAS is used as the background material which is mainly Cyclic-olefin copolymer. The main advantages of using TOPAS rather than other materials are (1) lower EML [α_{mat} =0.2 cm^{-1}] at f=1THz, (2) constant n=1.53, (3) it doesn't absorb water vapor.

9.3 Simulations & Our Findings

The simulation of our proposed fiber is done using the full vector finite element method (FEM) based software COMSOL, version 4.3b. For the representation of the structure, a perfectly matched layer (PML) is introduced and the thickness of the PML region used for the calculation is about 7.8% of the total fiber radius.

The calculation is done for different porosities. The porosities are taken as 61%, 71% and 81%. The power flow distribution at different porosities is shown in the fig 3. It is observed from the figure that as the core porosity increases the amount of mode power spreading into the core region of the PCF is increased.

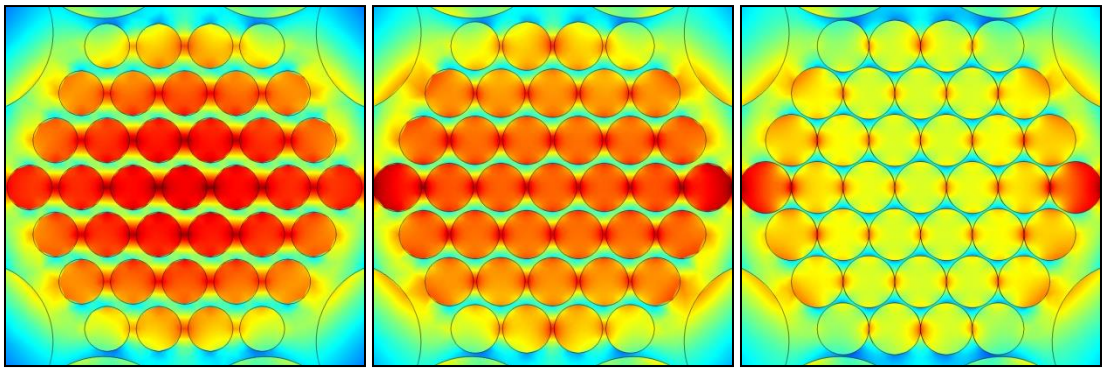

(a) (b) (c)

Fig 9.3: Power flow distribution of the proposed PCF of (a) 61%porosity (b) 71%porosity (c) 81%porosity

Unfortunately most of the researchers [26] put less focus to analyze the condition for single mode fiber which is considered as one of the most important factors for THz wave application. Before analyzing all the simulations, more attention was given to the condition of the single mode fiber. The single mode condition can be determined by the normalized frequency V parameter which can be calculated by

$$V = \frac{2\pi r f}{c}\sqrt{{n_{co}}^2 - {n_{cl}}^2} \leq 2.405, \quad \ldots\ldots\ldots\ldots \quad (1)$$

Where, r is the core radius, c is considered as the speed of the light in vacuum, f is the operating frequency, n_{co} and n_{cl} are the refractive indices of the core and the cladding respectively. The refractive index of the cladding n_{cl} is considered to be 1 as the cladding mostly contains the air holes and the refractive index of the air is 1. On the other hand, the core is porous core that's why its refractive index is considered to be same as the effective refractive index n_{eff}. For the existence of the single mode condition, the value of V parameter must be equal to or less than 2.405.

The variation of the V parameter with respect to different values of core diameter D_{core} and frequency is shown in the fig. 4 and fig. 5. It is observed from the figure that the V parameter is increased as core diameter and frequency is increased. The figure also represents the fact that the value of the V parameter does not exceed the value 2.405 and it satisfies the condition for single mode operation.

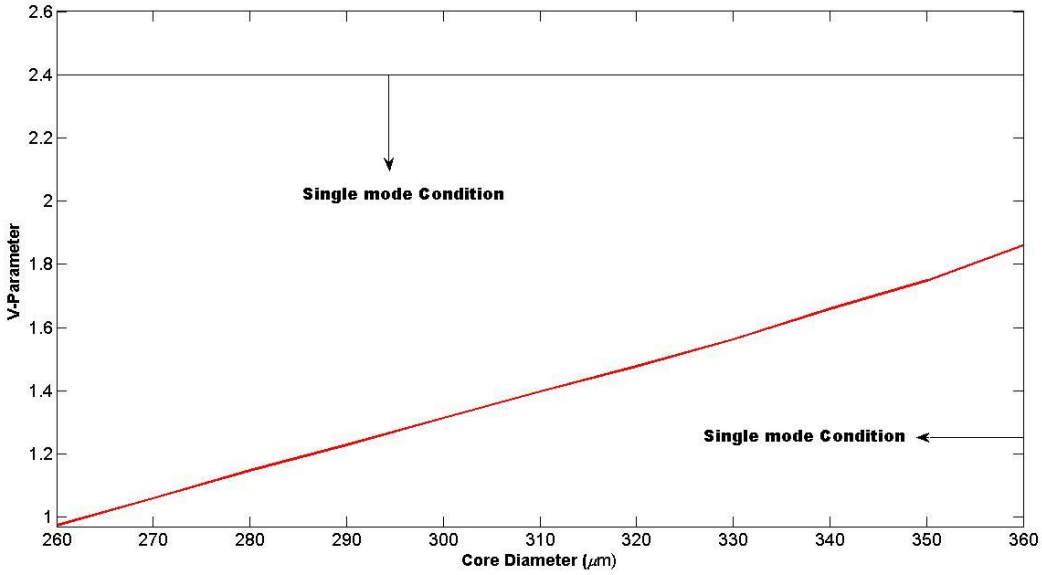

Fig 9.4: V parameter versus Core Diameter

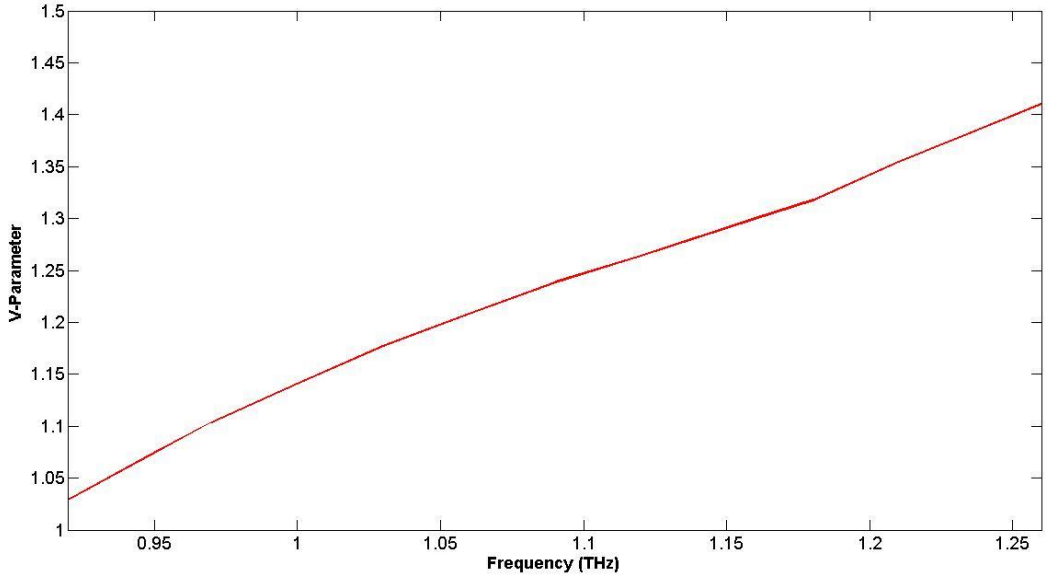

Fig 9.5: V parameter versus frequency

Before designing resourceful THz waveguide, four other major factors are needed to be considered. They are: Material absorption loss or effective material loss (EML), Fraction of mode power in the core, Confinement loss and the Chromatic dispersion.

Before staring the design our prime mindset was to reduce the EML and to get a maximum threshold value of the core power fraction. To reduce the EML, more focus is given to reduce the TOPAS material in the core. The material absorption loss can be calculated by

$$\alpha_{\text{eff}} = \sqrt{\frac{\varepsilon_0}{\mu_0}}\left(\frac{\int_{\text{mat}} n_{\text{mat}}|E|^2\alpha_{\text{mat}}\,\text{dA}}{\left|\int_{\text{all}} S_z\,\text{dA}\right|}\right) \qquad \ldots\ldots\ldots\ldots \quad (2)$$

Where, ε_0 and μ_0 are considered to be the relative permittivity and permeability in vacuum respectively, n_{mat} is the refractive index of TOPAS, α_{mat} is the bulk material absorption loss, ***E*** is the modal electric field and S_z is the z component of the pointing vector (S_z = ½(**E** × **H***).z), where **E** and **H** are the electric and magnetic fields respectively. The integration in the numerator of equation (2) is only performed over the solid material region (α_{mat}), while that in the denominator is perform over the entire region of the fiber. This is due the fact that air is transparent in THz region.

EML mainly depends on the amount of the material in the core and the material in the core depends on core porosity. To determine the porosity, Diameter of the air holes of the core is needed. As the core porosity increases the amount of air increases at the same time the amount of material decreases and consequently the EML decreases.

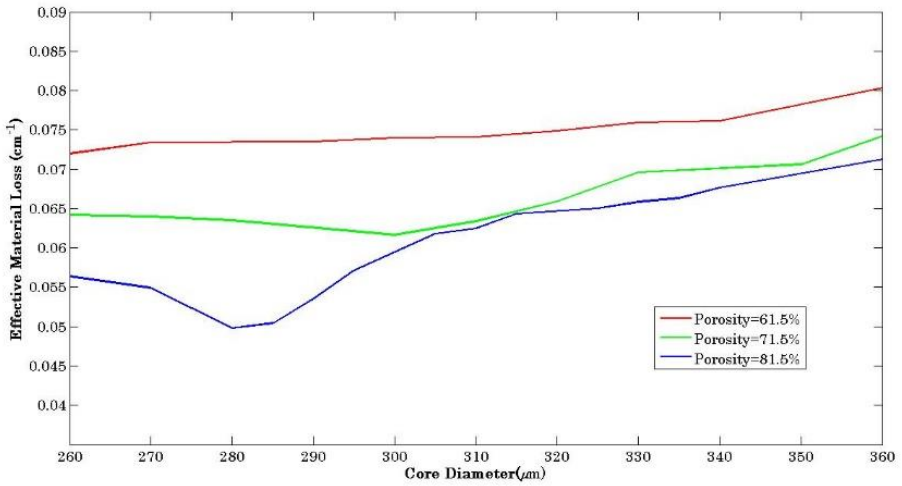

Fig 9.6: Effective material loss as a function of core diameter at different porosities

Figure 6 displays the EML as a function of D_{core} for different core porosity at constant frequency of 1.0 THz. It is seen from the figure that for same D_{core}, as the porosity increases the EML decreases. Porosity increases means filling more air into the core and it results less amount of material in the core which is responsible for the reduction of the EML.

It is very clear from the figure that at core porosity 81.5% material absorption loss is 0.04979 cm^{-1} for core diameter of 280 μm. This is due to the fact that the guided mode experiences less material and the core air-holes carrying most of the power. This result is obviously better than the previous result reported in Refs. [34], [29] and [28] and [28, 30, 31].

The figure 7 depicts the EML as a function of frequency f. It is seen that at 1.0 THz frequency minimum value of EML is found.

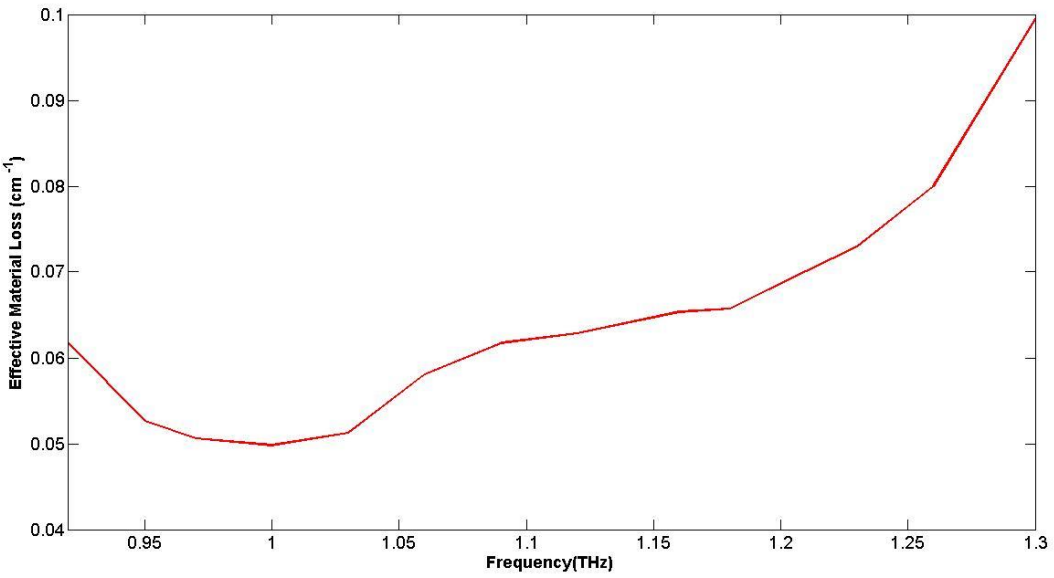

Fig 9.7: Effective material loss as a function of frequency

Another important parameter that must be considered before designing a standard THz waveguide is the amount of mode power propagation throughout the core air holes. The mode power propagation can be estimate

$$\eta' = \frac{\int_X S_z \mathrm{dA}}{\int_{\mathrm{all}} S_z \mathrm{dA}} \qquad \ldots\ldots\ldots\ldots \quad (3)$$

Where η' represents mode power fractionand X represents the area of interests. For designing a standard PCF it is necessary to flow the maximum amount of mode power throughout the core air holes.

The higher the core diameter (D_{core}), the higher the mode power fraction and the EML. Conversely reducing the D_{core} tends to reduce the EML and mode power fraction. These two factors are contradictory. So researchers must select an optimum value of the D_{core} to get the minimum EML and at the same time increased fraction of mode power. At 1.0 THz frequency and at 280 μm core diameter, minimum value of EML 0.04979 cm^{-1} and mode power fraction 43% is found.

The mode power fraction with the variation of frequency at 280 µm is shown in the figure 8, where it is observed that as the frequency increases the mode power fraction decreases and higher mode power is obtained at 1.0 THz.

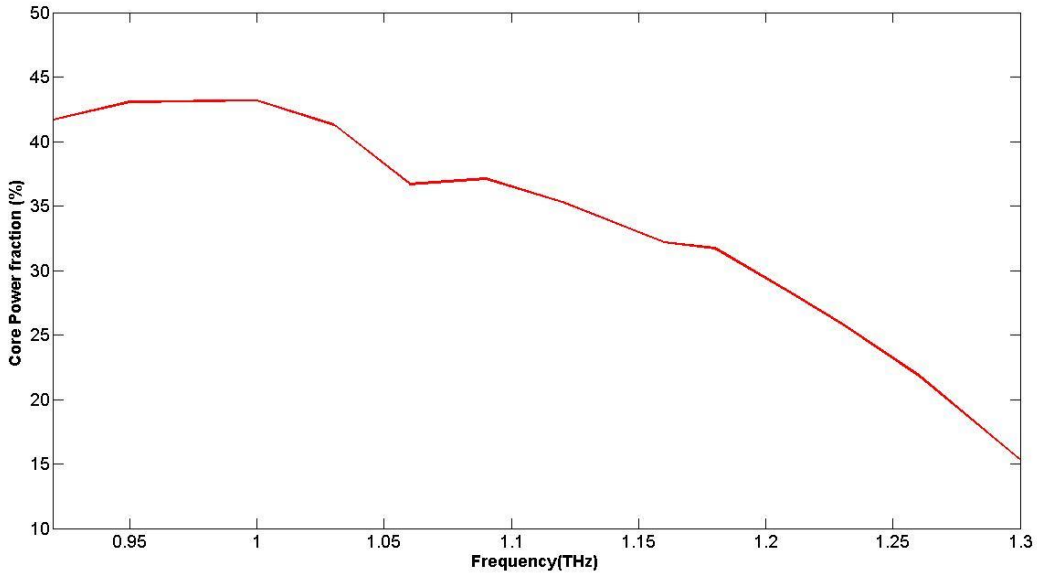

Fig 9.8: Fraction of mode power through the core air holes versus frequency

The figure 9 describes the changing of EML and fraction of mode power together with respect to change in the frequency. As the frequency increases, the EML increases and the fraction of mode power decreases.

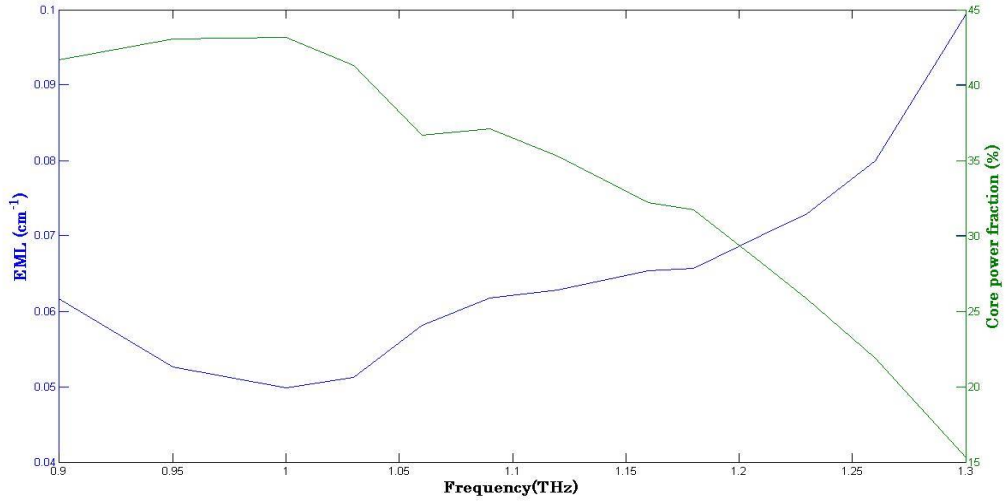

Fig 9.9: EML versus Frequency and Core power fraction versus Frequency

Confinement loss defines the ability of a PCF (photonic crystal fiber) to guide light with minimum loss. It causes due to the limited amount of cyclic cladding and can be can be calculated by taking the imaginary part of the complex refractive index. Confinement loss does not depend upon the core porosity or the core diameter but it depends on the number of air holes in the cladding. The more the number of air holes in the cladding, the lesser the confinement loss is found. So by increasing the number of air holes in the cladding, the confinement loss can be reduced. The confinement loss can be calculated by

$$\mathrm{LC} = 8.686\ (\frac{2\pi \mathrm{f}}{\mathrm{c}})\mathrm{Im}(n_{\mathrm{eff}})(^{\mathrm{dB}}/_{\mathrm{m}}) \qquad \text{.....} \quad (4)$$

Where, *f* is the frequency of the guiding light, *c* is speed of light in vacuum and Im (n_{eff}) symbolizes the imaginary part of the refractive index.

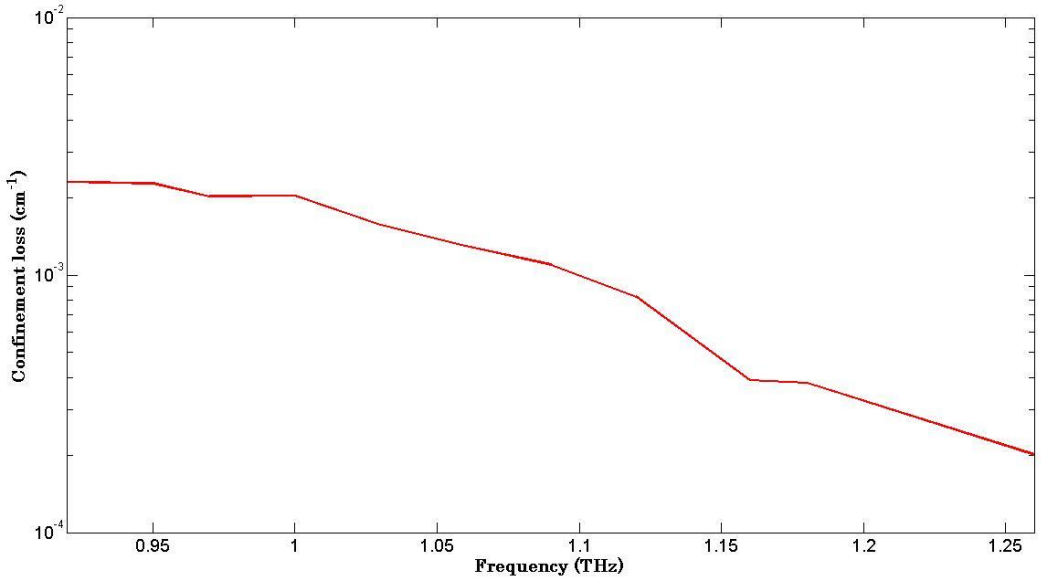

Fig 9.10 Calculated confinement loss at different frequencies

It is shown in the figure 9.10 that the confinement loss is a function of frequency. It is observed that as the frequency increases the confinement loss is scaled down which is much lower than the EML and that's why the confinement loss can be neglected. While calculating the confinement loss, the single mode condition must be carefully examined. In our proposed design, five rings of cladding are proposed. So, the confinement losses are calculated when the number of rings in the cladding is five. In order to reduce the confinement loss, number of rings in the cladding should be increased. From Ref. [35] it is known that increasing the number of the rings or diameter of air holes in the cladding, the dispersion properties of the material do not change significantly.

Dispersion is another important factor while concerning about the THz wave guidance. Now dispersion characteristics of the proposed PCF are discussed. As the refractive index of TOPAS is constant over the frequency range 0.1-1.5 THz [36]; the material

dispersion is ignored in this case and only the waveguide dispersion is analysed in this case. The waveguide dispersion can be calculated using the following equation [22],

$$\beta_2 = \frac{2}{c}\frac{dn_{eff}}{d\omega} + \frac{\omega}{c}\frac{d^2 n_{eff}}{d\omega^2} \quad \text{..... (5)}$$

Where w=2πf and c is the velocity of light in vacuum. In the figure 11 dispersion characteristics of the proposed fiber is shown.

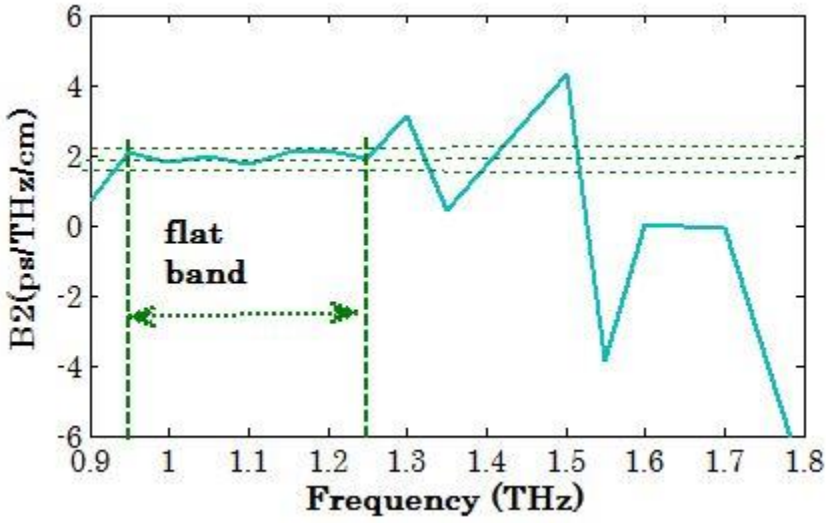

Fig 9.11: Dispersion Characteristics of the proposed PCF versus frequency

It can be seen that the variation of β_2 is less than 0.30 ps/THz/cm in the frequency range 0.95-1.25 THz. So it can be said that a flattened dispersion of 2.0±0.30 ps/THz/cm is gained over the frequency range 0.95-1.25 THz.

9.4 Fabrication

Fabrication is one of the most important factors after simulating the PCF. Previously, there are many problems regarding the fabrication. Recently the problem with the fabrication is removed and fabrication possibilities are greatly improved. There are different ways of fabrication. Stack and drilling method, capillary stacking, Sol-gel technologies and Extrusion techniques are most commonly used methods. Stack and drilling method is actually used for honeycomb and triangular lattices and is not authenticate to fabricate circular PCFs. In 2005, Bisen *et al.* reported a sol-gel technique [35] for micro and nano structure fabrication. Though Extrusion technique gives design freedom, its only limited to soft glasses. Ref. [31] proposes a capillary stacking technology which is actually suitable and versatile for PCF fabrication. Our proposed PCF can be fabricated using this capillary stacking technology where the dimensions like air–hole size, shape and spacing can be adjusted properly.

CHAPTER 10

DRAWBACKS & FUTURE PROPOSAL

An immensely lower effective material loss, notably marginal core power fraction, less confinement loss and near zero ultra-flat dispersion has been introduced in our proposed design. In our proposed design, single mode properties has also been satisfied and designed for THz wave guidance. For the first time Decagonal cladding and rotate hexagonal core has been introduced which helps us to reduce the effective material loss and preferably for a margin of core power fraction. Besides, higher air filling fraction and unique arrangement of five rings in the cladding helps to decrease the confinement loss. The primary implication of our proposed structure is its simplicity and loss reduction. Our proposed design contains attractive guiding properties which will be significant for THz wave application. For long distance communication of THz signal, our proposed design can be used relevantly.

The main drawback of our proposed design is power fraction can further be increased & EML can further be decreased. Still the accumulated result is satisfactory & can be developed in future for practical purpose.

So the future goal should be developing a fabrication process for this accumulated design which is efficient & easy so that worldwide it can be adopted. Furthermore, simulations should be continued for new designs so that low EML & high power fraction design can be adopted & fabricated practically.

References:

1. K. Wang and D. M. Mittleman, ‘‘Metal wires for terahertz wave guiding,’’ *nature* 432, 376–379 (2004).
2. B. Bowden, J. A. Harrington, and O. Mitrofanov, ‘‘Silver/polystyrene-coated hollow glass waveguides for the transmission of terahertz radiation,’’ *opt. lett.* 32(20), 2945–2947 (2007).
3. C. Themistos et al., “Characterization of silver/polystyrene (PS) coated hollow glass waveguides at THz frequency,” *J. Lightwave Technol.* 25(9), 2456–2462 (2007).
4. M. Skorobogatiy and A. Dupuis, “Ferroelectric all-polymer hollow Bragg fibers for terahertz guidance,” *Appl. Phys. Lett.,* vol. 90, no. 11, pp. 113514-1–113514-3, Mar. 2007.
5. L. J. Chen et al., “Low-loss subwavelength plastic fiber for terahertz waveguiding,” *opt. Lett.* 31(3), 308–310 (2006).
6. L.J.Chen, H.W. Chen, T.F.Kao, J.Y. Lu,and C.K. Sun,“Low-loss subwavelength plastic fiber for terahertz waveguiding*,” Opt. Lett.,* vol. 31, no. 3, pp. 308–310, Feb. 2006.
7. M. Nagel, A. Marchewka, and H. Kurz, “Low-index discontinuity terahertz waveguides,” *Opt. Express,* vol. 14, no. 21, pp. 9944–9954, 2006
8. L.J. Chen, H.W. Chen, T.F. Kao, J.Y. Lu, C.K. Sun, “Low-loss subwavelength plastic fiber for terahertz waveguiding”, *Opt. Lett.* 31 (3) (2006) 308–310.
9. C.S. Ponseca Jr., R. Pobre, E. Estacio, N. Sarukura, A. Argyros, M.C. Large, M.A. van Eijkelenborg, “Transmission of terahertz radiation using a microstructured polymer optical fiber”, *Opt. Lett.* 33 (9) (2008) 902–904.
10. K. Nielsen, H.K. Rasmussen, A.J. Adam, P.C. Planken, O. Bang, P.U. Jepsen, Bendable, “low-loss Topas fibers for the terahertz frequency range”, *Opt. Exp.* 17 (10) (2009) 8592–8601.
11. M. Goto, A. Quema, H. Takahashi, S. Ono, N. Sarukura, “Teflon photonic crystal fiber as terahertz waveguide”, *Jpn. J. Appl. Phys.* 43 (2B) (2004) L317–L319. pt.2.

12. G. Zhao, M.T. Mors, T. Wenckebach, P.C.M. Planken, “Terahertz dielectric properties of polystyrene foam”, *J. Opt. Soc. Amer. B* 19 (6) (2002) 1476–1479.
13. J.Y. Lu, C.P. Yu, H.C. Chang, H.W. Chen, Y.T. Li, C.L. Pan, C.K. Sun, “Terahertz air-core microstructure fiber”, *Appl. Phys. Lett.* 92 (6) (2008) 064105-1–064105-3.
14. M. Skorobogatiy, A. Dupuis, “Ferroelectric all polymer hollow Bragg fibers for terahertz guidance”, *Appl. Phys. Lett.* 90 (11) (2007) 113514-1–113514-3.
15. H. Han, H. Park, M. Cho, and J. Kim, “Terahertz pulse propagation in a plastic photonic crystal fiber,” *Appl. Phys. Lett.,* vol. 80, no. 15, pp. 2634–2636, 2002.
16. P.J.St. Russell, “Photonic crystal fibers”, *Science* 299 (5605) (2003) 358–362.
17. H. Han, H. Park, M. Cho, J. Kim, “Terahertz pulse propagation in a plastic photonic crystal fiber”*, Appl. Phys. Lett.* 80 (15) (2002) 2634–2636.
18. A. Hassani, A. Dupuis, M. Skorobogatiy, “Porous polymer fibers for low-loss terahertz guiding”, *Opt. Express* 16 (9) (2008) 6340–6351.
19. B. Ung, A. Mazhorova, A. Dupuis, M. Roze, M. Skorobogatiy, “Polymer microstructured optical fibers for terahertz wave guiding”, *Opt. Express* 19 (26) (2011) B848–B861.
20. K. Nielsen, H.K. Rasmussen, P.U. Jepsen, O. Bang, “Porous-core honeycomb bandgap THz fiber”, *Opt. Lett.* 36 (5) (2011) 666–668.
21. H. Bao, K. Nielsen, H.K. Rasmussen, P.U. Jepsen, “Fabrication and characterization of porous-core honeycomb bandgap THz fibers”, *Opt. Express* 20 (28) (2012) 29507–29517.
22. M. Uthman, B.M.A. Rahman, N. Kejalakshmy, A. Agarwal, K.T.V. Grattan, “Design and characterization of low-loss photonic crystal fiber”, *IEEE photonics J*. 4 (6) (2012).
23. S. Atakaramians, S. A. Vahid, B. M. Fischer, D. Abbott, and T. M. Monro, “Porous fibers: A novel approach to low loss THz waveguides,” *Opt. Exp.*, vol. 16, no. 12, pp. 8845–8854, Jun. 2008.
24. S. F. Kaijage, Z. Ouyang, and X. Jim, “Porous-core photonic crystal fiber for low loss terahertz wave guiding”, *IEEE Photon. Technol. Lett*., vol. 25, no. 15, pp. 1454–1457, Aug. 1, 2013.

25. M. Uthman, B.M.A. Rahman, N. Kejalakshmy, A. Agarwal, K.T.V. Grattan, “Design and characterization of low-loss photonic crystal fiber”, *IEEE photonics J.* 4 (6) (2012).

26. K. Nielsen, H. K. Rasmussen, P. U. Jepsen, and O. Bang, “Porous-core honeycomb bandgap THz fiber,” *Opt. Lett.*, vol. 36, no. 5, pp. 666–668, Mar. 2011.

27. M. Uthman, B.M.A. Rahman, N. Kejalakshmy, A. Agarwal, K.T.V. Grattan, Design and characterization of low-loss photonic crystal fiber, IEEE photonics J. 4 (6) (2012).

28. J. Liang, L. Ren, N. Chen, and C. Zhou, “Broadband, low-loss, dispersion flattened porous-core photonic bandgap fiber for terahertz (THz)- wave propagation,” *Opt. Commun.*, vol. 295, pp. 257 261, May 2013.

29. S. F. Kaijage, Z. Ouyang, and X. Jim, “Porous-core photonic crystal fiber for low loss terahertz wave guiding,”IEEE Photon. Technol. Lett., vol. 25, no. 15, pp. 1454–1457, Aug. 1, 2013.

30. Raonaqul Islam,G. K. M. Hasanuzzaman, Md. Selim Habib, Sohel Rana, M. A. G. Khan “Low-loss rotated porous core hexagonal single-mode fiber in THz regime”Elsevier Optical Fiber Technology 24 (2015) 38–43.

31. Sohel Rana, Golam Kibria, Md. Hasanuzzaman, Samiul Habib, Shubi F. Kaijage, Raonaqul Islam “Proposal for a low loss porous core octagonal photonic crystal fiber for T-ray wave guiding” Optical Engineering 53(11), 115107 (November 2014).

32. Md. Imran Hasan, S. M. Abdur Razzak, G. K. M. Hasanuzzaman, Md. Samiul Habib “Ultra-Low Material Loss and Dispersion Flattened Fiber for THz Transmission” IEEE PHOTONICS TECHNOLOGY LETTERS, VOL. 26, NO. 23, DECEMBER 1, 2014

33. Md.Saiful Islam , Sohel Rana, Mohammad Rakibul Islam, Mohammad Faisal, Hasan Rahman, Jakeya Sultana “Porous core photonic crystal fiber for ultra-low material loss in THz regime” IET Journals (July,2016)
34. . Nielsen, H. K. Rasmussen, A. J. L. Adam, P. C. M. Planken, O. Bang, and P. U. Jepsen, “Bendable, low-loss Topas fibers for the terahertz frequency range,” *Opt. Exp.,* vol. 17, no. 10, pp. 8592–8601, May 2009.
35. R. T. Bisen and D. J. Trevor, “Solgel-derived microstructured fibers: Fabrication and characterization,” in *Proc. Opt. Fiber Commun.Conf. (OFC)*, Mar. 2005, p. OWL6.
36. Raonaqul Islam, G.K.M. Hasanuzzaman, Md. Selim Habib, Sohel Rana, “Low-loss rotated porous core hexagonal single-mode fiber in THz regime,” *Optical Fiber Technology* , 38-43, May 2015.